The Plant Cell, Vol. 21: 1–20, November 2009, www.plantcell.org © 2009 American Society of Plant Biologists

Arabidopsis N-MYC DOWNREGULATED-LIKE1, a Positive Regulator of Auxin Transport in a G Protein–Mediated Pathway [W]

Yashwanti Mudgil,[a] Joachm F. Uhrig,[b] Jiping Zhou,[a] Brenda Temple,[c] Kun Jiang,[a] and Alan M. Jones[a,d,1]

[a] Department of Biology, University of North Carolina, Chapel Hill, North Carolina 27599
[b] Botanical Institute III, University of Cologne, D-50931 Cologne, Germany
[c] The R. L. Juliano Structural Bioinformatics Core Facility, University of North Carolina, Chapel Hill, North Carolina 27599
[d] Department of Pharmacology, University of North Carolina, Chapel Hill, North Carolina 27599

Root architecture results from coordinated cell division and expansion in spatially distinct cells of the root and is established and maintained by gradients of auxin and nutrients such as sugars. Auxin is transported acropetally through the root within the central stele and then, upon reaching the root apex, auxin is transported basipetally through the outer cortical and epidermal cells. The two Gβγ dimers of the *Arabidopsis thaliana* heterotrimeric G protein complex are differentially localized to the central and cortical tissues of the *Arabidopsis* roots. A null mutation in either the single β (AGB1) or the two γ (AGG1 and AGG2) subunits confers phenotypes that disrupt the proper architecture of *Arabidopsis* roots and are consistent with altered auxin transport. Here, we describe an evolutionarily conserved interaction between AGB1/AGG dimers and a protein designated N-MYC DOWNREGULATED-LIKE1 (NDL1). The *Arabidopsis* genome encodes two homologs of NDL1 (NDL2 and NDL3), which also interact with AGB1/AGG1 and AGG1/AGG2 dimers. We show that NDL proteins act in a signaling pathway that modulates root auxin transport and auxin gradients in part by affecting the levels of at least two auxin transport facilitators. Reduction of *NDL* family gene expression and overexpression of *NDL1* alter root architecture, auxin transport, and auxin maxima. AGB1, auxin, and sugars are required for NDL1 protein stability in regions of the root where auxin gradients are established; thus, the signaling mechanism contains feedback loops.

INTRODUCTION

Root architecture, which is the combination of root length and the position and density of lateral roots, is influenced by intrinsic and environmental signals and has become a model for studying developmental plasticity (Malamy, 2005). Any root architecture particular to the soil develops to maximize the efficiency of water and nutrient uptake. The length of the root is established primarily by the rate at which stem cells of the root apical meristem (RAM) produce cell derivatives but also by the rate at which those cell derivatives subsequently elongate (Beemster and Baskin, 1998; Ueda et al., 2005). The position and number of lateral roots is established by paracrine (cell to nearby cell) signals originating from vascular cells designated xylem elements (Dubrovsky et al., 2000, 2001), by the position within a gradient of the plant hormone auxin, and by nutrients including sugars, minerals, and some amino acids (Lejay et al., 1999; Forde, 2002; Gibson, 2005; Forde and Lea, 2007; Gutierrez et al., 2007; Karthikeyan et al., 2007; Zhang et al., 2007; Peret et al., 2009; Rubio et al., 2009). Lateral roots form through a concerted set of cell divisions of a founder cell population within a tissue called the pericycle that abuts the central vascular cylinder (Malamy and Benfey, 1997).

Arguably, the best understood signal determining root architecture is auxin. The dynamic flow and gradient of auxin is established, in part, by polarized transport from the aerial tissues down through the central cylinder of vascular cells of the root to the root tip and by auxin synthesized by the root apex (Petersson et al., 2009). This so-called acropetal auxin transport becomes basipetally oriented after it reaches the root tip where it then travels back toward the shoot through the outer cortical cells of the root (Jones, 1998). The position and activity of a small family of membrane proteins designated PIN-formed (PIN) proteins are critical for this pattern of auxin flux (Blilou et al., 2005; Petrasek et al., 2006; Wisniewska et al., 2006; Zazimalova et al., 2007; Mravec et al., 2009) and together with autonomous auxin synthesis at the root tip and auxin deactivation reactions at other locations, polarized auxin transport drives a defined auxin gradient with predicted localized maxima (Grieneisen et al., 2007; Petersson et al., 2009). This auxin gradient pattern changes in response to signals, such as gravity, touch, and presumably other environmental cues, resulting in different root architecture (Forde, 2002; Malamy, 2005; Forde and Lea, 2007). Despite the importance of manipulating root architecture for agricultural benefit and its use as a model for developmental plasticity, the complete molecular network for any of these pathways affecting root architecture remains incomplete.

[1] Address correspondence to alan_jones@unc.edu.
The author responsible for distribution of materials integral to the findings presented in this article in accordance with the policy described in the Instructions for Authors (www.plantcell.org) is: Alan M. Jones (alan_jones@unc.edu).
[W] Online version contains Web-only data.
www.plantcell.org/cgi/doi/10.1105/tpc.109.065557

Previously, we showed that the heterotrimeric G protein couples unidentified signals in the *Arabidopsis thaliana* root to elements regulating cell proliferation and lateral root primordia formation (Ullah et al., 2001, 2003; Chen et al., 2006a; Trusov et al., 2007). Furthermore, we presented a working model whereby (1) the G protein heterotrimeric complex acts to attenuate cell proliferation in the RAM, (2) the activated Gα subunit (*Arabidopsis* GPA1) stimulates cell proliferation in the RAM by shortening the G1 phase of the cell cycle, and (3) the Gβγ dimer reduces cell division in the pericycle tissue possibly by blocking reentry into the cell cycle. This action involves, in part, transcriptional regulation since the Gβγ dimer represses ~25% of the auxin-induced genes in the root, including genes essential for lateral root development (Ullah et al., 2003).

It is well established in animals that upon activation of the heterotrimeric G protein complex and the consequent release of the Gβγ dimer from the complex, Gβγ interacts with cognate cytoplasmic effectors to propagate signaling that is initiated extracellularly. The importance of Gβγ in the propagation of signaling has been firmly established in plants; however, not a single cognate Gβγ effector has been identified. While mammals have five Gβ subunits and 12 Gγ subunits, *Arabidopsis* has a single gene encoding Gβ (*AGB1*) and at least two genes encoding Gγ subunits (*AGG1* and *AGG2*). Well-known Gβγ effectors in animals are phosducin, potassium channels, phospholipases, adenyl cyclases, mitogen-activated protein kinases, and phosphoinositol-3-kinase (Crespo et al., 1994; Tsukada et al., 1994; Xu et al., 1995; Akgoz et al., 2002; Zhao et al., 2003; Kino et al., 2005; Rebois et al., 2006; Chen et al., 2008).

Characterization of *agb1*, *agg1*, and *agg2* null mutants revealed that there is considerable phenotypic overlap and that AGB1/AGG dimers propagate signaling in various physiologies, including cell division, lateral root development (Chen et al., 2006a), biotic and abiotic stress (Booker et al., 2004; Trusov et al., 2006; Wang et al., 2007), hormone signaling (Ullah et al., 2003; Pandey et al., 2006; Chen et al., 2009), and touch sensing (Weerasinghe et al., 2009). Recent detailed analysis of these mutants also points to the significant differences between them, raising the possibility that *Arabidopsis* GPA1 and AGB1 can act independently of AGG1/AGG2 or that there exists undiscovered AGG subunits in *Arabidopsis* (Trusov et al., 2008).

Although it is well established that various pathways (e.g., auxin, abscisic acid, D-glucose, jasmonic acid, fungal defense, and O_3) are modulated by AGB1/AGG signaling, the molecular components of Gβγ signaling remain recondite (Temple and Jones, 2007; Ding et al., 2008). Some of the specificity for this myriad of signaling pathways is imparted by tissue-specific expression of the *AGG* subunits. For example, while *AGB1* has a broad expression pattern throughout the root, *AGG1* is expressed within the stele, while *AGG2* is expressed in the root cortex. Because of differences in lateral root phenotypes between null mutants of *agg1* and *agg2*, Trusov et al. (2007) proposed earlier that the AGG subunits provide functional selectivity that, in concert with AGB1, acts as a negative regulator of lateral root formation in specific root layers.

AGB1/AGG regulates multiple developmental processes (Lease et al., 2001; Ullah et al., 2003; Peskan-Berghofer et al., 2005; Chakravorty and Botella, 2007). To identify the components of AGB1/AGG signaling, we performed yeast interaction mating using the AGB1/AGG2 dimer as a bait to screen for physical interactors in *Arabidopsis* cDNA expression libraries. We found a protein designated here as N-MYC DOWNREGULATED-LIKE1 (NDL1), which is similar to mammalian N-myc Downregulated (NDR) proteins, although the precise molecular function of NDR proteins is unclear (Zhou et al., 2001; Qu et al., 2002).

In plants, an NDR-like protein (SF21) was originally reported from sunflower (*Helianthus annuus*) as a transmitting tissue and pollen-localized protein, but no function was revealed (Krauter-Canham et al., 1997). SF21 is a member of a multigene family showing multiple alternative and organ-specific splicing transcripts (Lazarescu et al., 2006) and ubiquitous expression in all plant organs, suggesting a housekeeping functionality.

In this article, we report the following. (1) NDL proteins interact with the AGB1/AGG1 and AGB1/AGG2 dimers in *Arabidopsis* and that this interaction is evolutionarily conserved. (2) NDL proteins are positive effectors of primary root growth and lateral root formation. (3) NDL proteins positively modulate basipetal and negatively modulate acropetal auxin transport in an AGB1-dependent manner. (4) NDL1 together with AGB1 regulate primary root length and lateral root density through modulation of auxin transport possibly by regulating auxin transport carrier proteins like PIN2 and AUX1. (5) Steady state NDL1 protein level is dependent on auxin in a concentration-dependent manner and dependent on the presence of AGB1, auxin, and D-glucose, indicating a feedback mechanism of action.

RESULTS

NDL Proteins Are Novel Interacting Partners of AGB1 and *Arabidopsis* Regulator of G Protein Signaling Protein

We identified a novel AGB1/AGG2 interacting protein using a stream-lined, yeast three-hybrid protein complementation assay wherein the AGB1/AGG2 dimer served as bait to interrogate three *Arabidopsis* cDNA prey libraries. One candidate interactor, designated NDL1, was confirmed by cotransformation of yeast strain AH109 with individual bait and prey constructs. NDL1 also interacted with AGB1/AGG1 in yeast (Figure 1A). Mouse NDRG1 interacted with plant AGB1/AGG1 and AGB1/AGG2 (Figure 1A), suggesting that this interaction is evolutionarily conserved throughout metazoans. Protein interaction was detected in yeast irrespective of the presence or absence of Met in the media (Figure 1A). Because expression of AGG2 from the bait vector is repressed by Met, this interaction in the absence of AGG2 suggests either that the physical interaction with AGB1 does not involve a Gγ subunit or that the yeast Gγ subunit (Ste18) complements the loss of AGG1/AGG2 in the presence of Met. Typically, Gβ subunits are unstable in the absence of Gγ. Therefore, for simplicity, we will refer to NDL1 here as an AGB1/AGG-interacting protein, while recognizing that we have only formally shown that NDL1 interacts with the AGB1 subunit.

Coimmunoprecipitation demonstrated that NDL1 and AGB1 proteins can physically interact in planta (Figure 1B). *Nicotiana benthamiana* leaves were coinfiltrated with plasmids expressing

A

Bait+Prey	Growth on -W-L-H-Ade	Growth on -W-L-M-H	Xgal stain -W-L-H-Ade	Xgal stain -W-L-M-H
NDL1+AGB1AGG2	+	+	+	+
NDL2+AGB1AGG2	+	+	+	+
NDL3+AGB1AGG2	+	+	+	+
NDRG1+AGB1AGG2	+	+	+	+
NDL1+AGB1 AGG1	+	+	+	+
NDL2+AGB1 AGG1	+	+	+	+
NDL3+AGB1+AGG1	+	+	+	+
NDL1+RGS1-C4	+		+	
NDL2+RGS1-C4	+		+	
NDL3+RGS1-C4	+		+	
NDRG1+RGS1-C4	+		+	
	-W			-W
	+			-
AGB1+AGG2	+			-
AGB1+AGG1	+			-
RGS1-C4	+			-

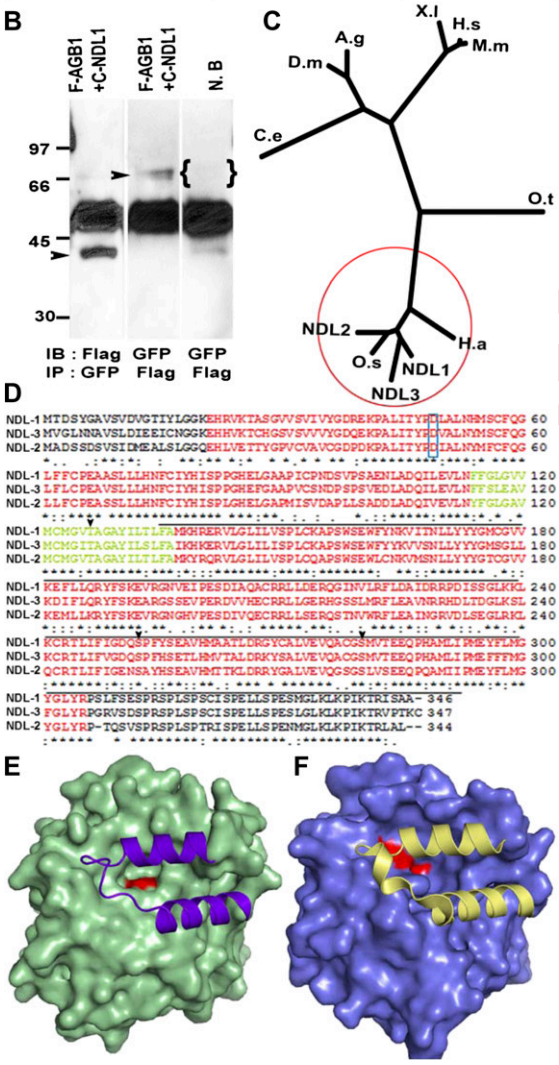

Figure 1. Protein Interaction, NDL Gene Family, and Putative Orthologs, and NDL and Similar Protein Structure.

the coding regions of *AGB1* and *NDL1* fused with FLAG and cyan fluorescent protein (CFP) epitopes, respectively (noted as F-AGB1 and C-NDL1 in Figure 1B). Immunoprecipitation with antibodies to green fluorescent protein (GFP) coimmunoprecipitated FLAG-tagged AGB1, and immunoprecipitation with anti-FLAG antibodies coimmunoprecipitated CFP-tagged NDL1 protein (Figure 1B, lanes 1 and 2, arrowheads); no specific protein was immunoprecipitated when extracts from untransformed tobacco leaves were used (Figure 1B, lane 3, brackets). We also used a glutathione *S*-transferase (GST)-tagged version of NDL1 for immunoprecipitation with FLAG-tagged AGB1 and found that anti-FLAG antibodies coimmunoprecipitated GST-tagged NDL1 (see Supplemental Figure 1 online). [AQ2]

(A) Yeast strain AH109 was transformed with two plasmids: the pBridge (DNA-BD) vector containing *AGB1/AGG1* or *AGB1/AGG2* and the Gal4ACTD conjugated construct having *NDL1*, *NDL2*, *NDL3*, or NDRG1 (mouse NDRG1). The cells were grown on SC medium lacking Trp, Leu, His, and adenine (-W-L-H-Ade) or SC-W-L-H medium minus Met to repress *AGG* expression (-W-L-M-H). All three NDL proteins interacted with AGB1+AGG2/or AGG1 in a yeast three-hybrid assay. Interactions were scored on the basis of activation of the *HIS3* reporter gene, X-gal staining, and presence or absence of Met. Single-domain controls: strain AH109 was transformed with single-domain plasmids alone and grown on selection. Using the same approach, the interactions of the prey set were also tested against the C-terminal cytoplasmic domain (C4) of *Arabidopsis* RGS1.

(B) AGB1 and NDL1 interaction in planta. After 22 h of *Agrobacterium tumefaciens*–mediated transient expression of *FLAG:AGB1* (F-AGB1) and *CFP:NDL1* (C-NDL1) in wild-type *N. benthamiana* leaves, total protein was isolated and was immunoprecipitated with anti-FLAG (for AGB1) and anti-GFP (for NDL1) antibodies. Immunoprecipitated (IP) proteins were detected by immunoblotting with the indicated antibody (IB). Lane 1, IP of NDL1 with anti GFP antibodies; lane 2, IP of AGB1 with anti FLAG antibodies; lane 3, wild-type *N. benthamiana* extract (N.B) IP with anti FLAG. NDL1 coimmunoprecipitates with AGB1, and the reciprocal coimmunoprecipitation also occurred (lanes 1 and 2). Arrowheads indicate the position of NDL1 and AGB1. Brackets highlight the absence of AGB1 in the control. Protein masses are indicated at the left side of the immunoblots (in kilodaltons).

(C) Phylogenic tree of NDR proteins: all plant NDR homologs form a separate group in the unrooted tree and are highlighted by the red circle (X.l, *Xenopus laevis*; H.s, *Homo sapiens*; M.m, *Mus musculus*; A.g, *Anopheles gambiae*; H.a, *Helianthus annuus*; O.t, *Ostreococcus tauri*; O.s, *Oryza sativa;* D.m, *Drosophila melanogaster*; C.e, *Caenorhabditis elegans*). The phylogenetic tree was calculated with MrBayes as described in Methods.

(D) NDL proteins are highly similar with conserved domains: amino acid alignment of the three *Arabidopsis* NDL proteins shows that all three NDL proteins contain the conserved NDR domain (red), an overlapping α/β hydrolase fold (underlined), a conserved Asp (boxed), a conserved hydrophobic patch (green), and catalytic triad residues marked with arrowheads.

(E) Atomic model of NDL1: Surface representation (light green) of the active site pocket in NDL1 with overlaying flap (purple). Conserved D (TYP**D**) in pocket is colored red.

(F) Surface representation (violet) of the active site pocket in the 2PU5 template with the overlying flap in yellow. Active site residues (S112, D237, and H265) are colored red.

Arabidopsis Regulator of G Protein Signaling (RGS1) is a seven-transmembrane protein known to interact with GPA1. Therefore, we tested RGS1 interaction with NDR proteins from *Arabidopsis* and mouse. The C-terminal domain of RGS1 (249 to 459 amino acids), which was previously shown to interact with GPA1, was cloned as bait (Chen et al., 2003; Johnston et al., 2007; Grigston et al., 2008). NDL1, NDL2, NDL3, and mouse NDRG1 interacted with the C-terminal domain of RGS1 in the yeast two-hybrid configuration (Figure 1A), raising the possibility that RGS1 is a candidate seven-transmembrane receptor in AGB1/NDL-mediated signaling.

NDL Proteins from Plants Are Similar to Each Other and Are Predicted Members of a Lipase Superfamily Containing an NDR Domain and an α/β Hydrolase Fold

NDL1 sequence similarity drops from ~70% among plants to ~30% between plants and other organisms. For example, NDL1 has 48% similarity and 29 to 30% identity with human homologs NDR1, NDR2, and NDR3 (see Supplemental Figure 2 online). The *Arabidopsis* genome encodes two additional proteins (designated here as NDL2 and NDL3) sharing ~75% amino acid identity with NDL1. As with NDL1, both NDL2 and NDL3 showed positive interaction with AGB1/AGG (Figure 1A), suggesting that all members of the NDL family could participate in Gβγ signaling. Phylogenetic analysis revealed that all plant NDR-like members form a clade separate from other eukaryotic NDR proteins in an unrooted tree (Figure 1C, red circle; see Supplemental Figure 2 and Supplemental Data Set 1 online). All plant NDL protein sequences except the one from the alga *Ostreococcus tauri* share >70% identity. For example, NDL1 is 74 and 75% identical, respectively, to putative orthologs in rice (*Oryza sativa*) and sunflower, whereas *O. tauri is* only 33% identical with *Arabidopsis* NDL1. All three *Arabidopsis* NDL proteins have an NDR domain (Figure 1D, red residues), an α/β hydrolase fold (Figure 1D, underlined residues), a conserved hydrophobic patch of 23 amino acids (Figure 1D, green residues), and a conserved Asp (Figure 1D, boxed). The presence of all of these features strongly suggests that the plant NDL proteins belong to the NDR protein family.

More specifically, domain searches of NDL1 using various databases (see Methods) predict NDL1 to be a member of the esterase/lipase superfamily. Members containing the NDR domain are found in a wide variety of multicellular eukaryotic proteins, although the precise molecular function of members of this family is unknown. The α/β hydrolase fold is common to several hydrolytic enzymes of different origin and catalytic function (Ollis et al., 1992).

The consensus fold determined by the BioInfoBank Meta-Server (http://meta.bioinfo.pl/) for NDL1 was that of an α/β hydrolase (Renault et al., 2005). All 20 of the top MetaServer candidates were different α/β hydrolase structures, with little variation in the 3-D Jury consensus score (Ginalski et al., 2003). Homology models based on the templates identified by the MetaServer were built using the Insight-II Molecular Modeling System (www.accelrys.com) and then evaluated for structural integrity using the Profiles-3D module. Scores above 0.1 indicate valid protein structures, while higher scores indicate more accurate predicted structures with high confidence. Correct experimental structures score near 1.0. The normalized Profiles-3D score ranged from 0.17 for the model based on template 1WOM.pdb (Kaneko et al., 2005) to 0.55 for the model based on template 2PU5.pdb (Horsman et al., 2007). The model with the highest Profiles-3D score had the better fold and was selected as the final structural model for the NDL1 protein (Figure 1E). The resulting molecular model lacks the characteristic catalytic triad that provides the basis of enzymatic activity of the α/β hydrolase superfamily. For comparison, the template 2PU5.pdb (protein BphD of the bacteria *Burkholderia xenovorans*) containing the catalytic triad S112, D237, and H265 is shown (Figure 1F, colored red). At the conserved S, D, H triad of the α/β hydrolase model T, S, S, respectively, was found in NDL1 (Figure 1D, arrowheads). Although the catalytic triad is missing, the NDL1 protein model has a catalytic pocket and a conserved Asp within this pocket (TYP**D**xALN, Figures 1D, boxed, and 1E, red). This Asp residue is conserved in all NDR proteins (see Supplemental Figure 2, red arrow for conserved D). There is an overlying hydrophobic patch/flap covering the catalytic pocket (Figure 1E, purple). Recombinant NDL1 protein lacked reproducible lipase or esterase activity under conditions described in Methods using two standardized esterase lipase assays (Furukawa et al., 1982; Yang et al., 2002).

NDL1 Is a Ubiquitously Expressed Gene Encoding a Cytoplasmic Protein with Informative Protein Distribution Patterns in Roots

Searches of public databases of *NDL1* gene expression profiles revealed high (values ≥7000) ubiquitous expression with a relative maximum in pollen (see Supplemental Figures 3A and 3B online). Both *AGB1* and *NDL1* genes showed a similar relative distribution of expression among tissues. *AGB1* gene expression, albeit at 10-fold lower levels, overlapped the *NDL1* expression profile (see Supplemental Figure 3B online). *NDL2* and *NDL3* overall had patterns of expression that were different from that of *NDL1*. For example, *NDL3* showed maximum expression in the shoot apex (see Supplemental Figure 3B online).

Quantitative real-time PCR (qRT-PCR) analysis of mRNA isolated from different organs confirmed expression of *NDL1* in reproductive (flower) as well as vegetative (stem, root, and leaves) tissues with highest expression in flowers (see Supplemental Figure 3C online).

Spatial localization of the steady state levels of NDL1 protein at the tissue level were investigated using translational fusions with β-glucuronidase (GUS). Data from at least three independent, translational fusion lines were analyzed, and representative patterns are shown in Figure 2. NDL1 was observed at the radicle and young root tips (Figure 2A, arrow) and at higher steady state levels in emerging cotyledons at the base of the root-shoot junction (Figure 2B, arrow, 2- to 3-day-old seedling). Ten-day-old, light-grown leaves showed high levels in veins, ground tissue (Figure 2C; see Supplemental Figures 3D and 3E online), stipules, and at the base of trichomes (Figures 2D and 2E). Detailed cellular analysis of leaf tissue showed high NDL1 levels in the vasculature as well as in the mesophyll; however, NDL1 was absent from stomata (see Supplemental Figures 3D and 3E online, see arrows, transverse and oblique paradermal

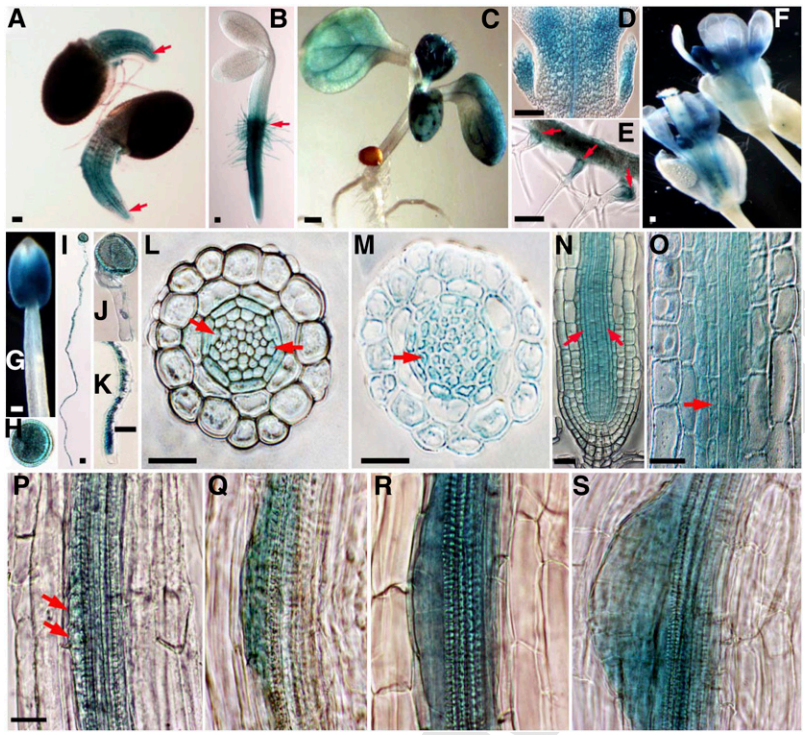

Figure 2. NDL1 Tissue and Organ Localization.

(A) to **(S)** In situ localization of NDL protein was indirectly determined using translational NDL-GUS fusion lines (T3). Bars = 50 μm in **(A)** to **(G)** and **(I)**, 20 μm in **(L)** to **(S)**, and 10 μm in **(H)**, **(J)**, and **(K)**. **(P)** to **(S)** have the same magnification for direct comparison.
(A) One- to two-day-old seedlings with emerging radicle. Arrow indicates staining at the root tip.
(B) Two- to three-day-old, light-grown seedling. Arrow indicates staining at the root-shoot junction.
(C) Ten-day-old, light-grown plant.
(D) Stipules at the leaf base.
(E) Mature true leaf, with red arrows showing localization at the base of trichomes.
(F) Mature flower.
(G) Stamen.
(H) GUS-stained and fixed mature pollen grain.
(I) Germinated GUS-stained and fixed pollen grain.
(J) Head of the germinated GUS-stained and fixed pollen grain at higher magnification.
(K) Tip of the germinated GUS-stained and fixed pollen grain at higher magnification.
(L) Cross section of the primary root tip region; red arrows indicate comparatively deep staining at the endodermal layer.
(M) Cross section of primary root around basal meristem.
(N) Longitudinal section of primary root showing apical and basal meristematic zones.
(O) Longitudinal section of primary root from the basal meristem region (marked by red arrows in **[N]**) at higher magnification.
(P) Stage I of lateral root primordium development; red arrows point toward individual cells in layer.
(Q) Stage II of lateral root primordium development.
(R) Stage III of lateral root primordium development.
(S) Stage IV of lateral root primordium development.

section of mature leaf). In soil-grown mature plants, GUS staining was detected in flowers, specifically in mature stamens, in various regions in the cytoplasm of the dry and germinating pollen grains (Figures 2F to 2K).

An informative localization pattern was observed around the meristem in the root. Histochemical GUS staining in the primary and lateral root tips showed strong staining for NDL1 protein in the quiescent center (see Supplemental Figure 3F online, arrow) and other cell layers in the central elongation zone, with a relatively higher level in the endodermis and pericycle (Figures 2L to 2O, red arrows pointing to pericycle). A gradient of NDL1-GUS staining was observed to be the highest in the central elongation zone in all the cell layers (Figure 2O; see Supplemental Figure 3F online) and decreasing from the endodermal layer toward the differentiation zone. Steady state NDL1 protein level was high within the vasculature in the upper parts of the mature root (see Supplemental Figure 3G online). NDL1 localization was observed in the initial stages of lateral root primordia formation (Figures 2P to 2S, stage I to IV, arrows pointing toward new cells generated by anticlinal divisions). Similar layer-specific patterning was

observed for lateral roots (see Supplemental Figure 3H online). This pattern of localization was similar to *AGB1* expression (Chen et al., 2006b; Trusov et al., 2008).

In silico prediction of the subcellular localization of NDL1 using TargetP (Emanuelsson et al., 2000) reported that this protein lacks obvious organelle targeting sequences. Expression of C-terminal, GFP-tagged *NDL1* under the transcriptional control of the *NDL1* promoter (ProNDL1-*NDL1-GFP*) showed localization of this protein in punctate cytoplasmic structures (Figure 3A, arrows). The cytoplasmic localization of NDL1 was further confirmed by transiently expressing (35S-*NDL1*) N- and N/C-terminal GFP fusions (Karimi et al., 2002) in tobacco (*N. benthamiana*; Figures 3E and 3F). In addition, the similar localization pattern of both N- and C-tagged NDL1 in *Arabidopsis* epidermal and in tobacco pavement cells (Figure 3) suggest that the NDL1 localization is determined by a sequence internal to NDL1 proteins, driven by interaction with the membrane-delimited Gβγ dimer.

AGB1 Is Essential for Posttranslational Protein Stability of NDL1 in the Root Meristems

Both NDL1 protein and *AGB1* transcript were at their highest level in the RAM during the early stages of development (Figures 4A to 4F), but unlike NDL1, *AGB1* was not more prominently expressed in the distal endodermal and pericycle layers (cf. arrows in Figures 2L and 4B to brackets in 4E). The diffuse stele expression of *AGB1* confirms the results of Trusov et al. (2007). Lateral roots showed *AGB1* expression in the meristematic zone and distal elongation zone and in the vasculature of the mature lateral root (Figure 4F; see Supplemental Figure 4B online), a pattern that overlapped NDL1 protein distribution (Figure 4C; see Supplemental Figures 3H and Figure 4A online).

Since NDL1 localization shares nearly the same regions of the root tip as *AGB1* expression and because AGB1 and NDL1 physically interact, we hypothesized that NDL1 requires its partner, AGB1, either to regulate *NDL1* levels or to be stable posttranslationally. Therefore, we determined the level of *NDL1* gene expression in the absence of *AGB1* (*agb1-2*, described in Ullah et al., 2003) using qRT-PCR and found that *NDL1* expression levels were similar to those in the wild type (Figure 5D). In order to study any posttranslational effect, we determined the level of NDL1 protein in the absence of AGB1. In early stages of root development in *agb1-2* roots, NDL1 was excluded from the primary root tip although still expressed at the root-shoot junction (cf. bracket in Figure 4A with that in Figure 4G; cf. Figures 4B and 4H). NDL1 protein was only weakly detectable in lateral root primordia (Figure 4I) and elongated roots (see Supplemental Figures 4C and 4D online) in *agb1-2*. This indicates that AGB1 is required for a high steady state level of NDL1 protein around the primary and lateral root meristems. Note that NDL1 protein was at normal levels in other root tissues lacking AGB1. For example, vasculature of mature roots showed detectable NDL1 protein levels in *agb1-2* roots (Figure 4I; see Supplemental Figures 4C and 4D online). The nonspecific protease inhibitor MG132 (100 μM, 4 h) restored NDL1 protein levels close to wild-type levels in the primary root (cf. Figures 4B and 4J), and the lateral root showed restoration of protein stability to a level lower than that of the wild type after 4 h of treatment (cf. Figures 4C and 4K). The latter results suggest that AGB1 has a role in posttranslational stability of NDL1.

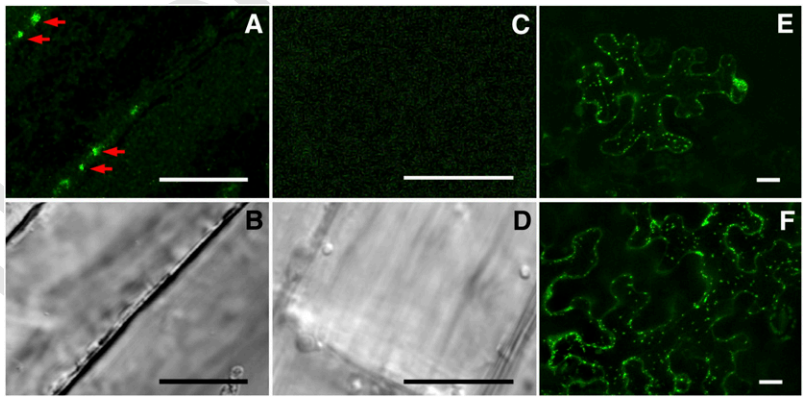

Figure 3. NDL1 Subcellular Localization.

(A) Laser scanning confocal micrographs showing cytoplasmic localization of C-terminally GFP-tagged *NDL1* stably expressed in *Arabidopsis* root epidermal cells under the transcriptional control of the *NDL1* promoter.

(B) Corresponding differenetial interference contrast image to the image shown in **(A)**.

(C) Control epidermal cell not expressing a GFP-tagged *NDL1*.

(D) Corresponding differenetial interference contrast image shown in **(C)**. Bars = 10 μm in **(A)** to **(D)**.

(E) and **(F)** Spinning disc confocal micrographs showing cytoplasmic localization of N-terminally **(E)** and N- plus C-terminally GFP-tagged **(F)** 35S-*NDL1* transiently expressed in *N. benthamiana*. Bars = 20 μm.

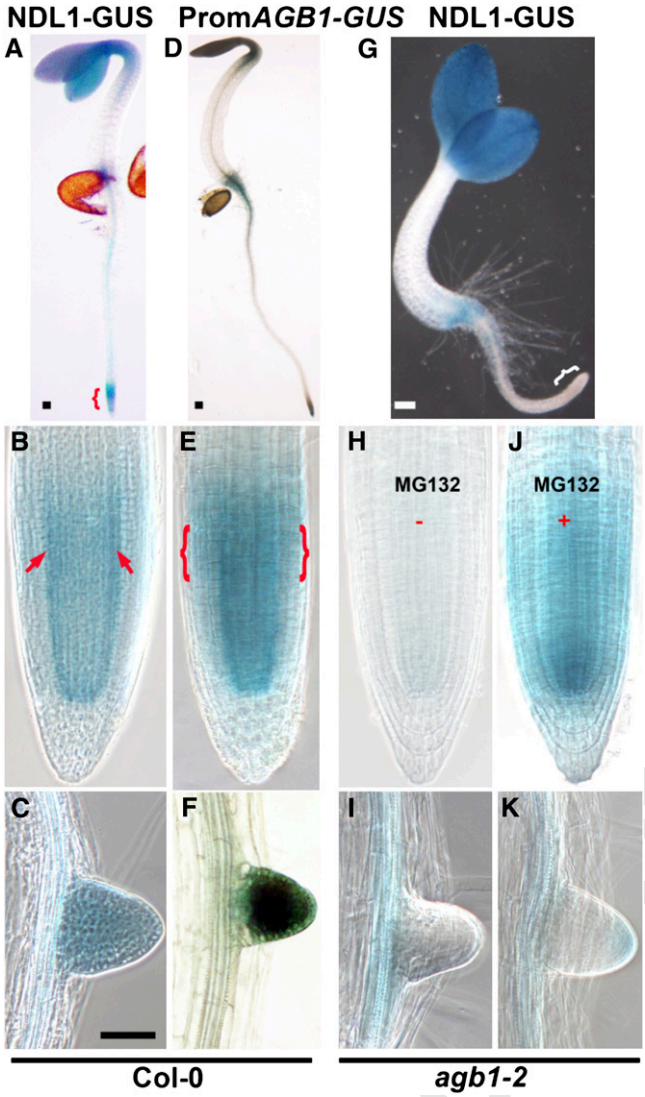

Figure 4. In Vivo Localization Pattern of NDL1 Protein in the Root in the Presence and Absence of AGB1.

(A) NDL-GUS staining pattern in the wild-type seedling. Bracket indicates area shown in **(B)**.
(B) NDL1-GUS staining pattern in wild-type root tip.
(C) Lateral root staining pattern of NDL1 in wild-type (Col-0) background.
(D) Transgenic plant expressing transcriptional fusion of the *AGB1* promoter with *GUS*.
(E) *AGB1* expression in the root tip.
(F) Lateral root primordium expression of *AGB1*.
(G) NDL1-GUS staining pattern in the *agb1-2* background.
(H) Lateral root staining pattern of the steady state level of NDL1 in the *agb1-2* background. NDL1 was not detectable (−) around the RAM in primary and lateral roots in the absence of AGB1. Compare the bracketed region of **(A)** to the bracketed region of **(G)**, and **(B)** and **(H)** for an enlarged view.
(J) and **(K)** MG132 treatment (100 μM for 4 h) of 4-d-old seedling resulted in reappearance of NDL protein (+) in the primary and lateral roots in the *agb1-2* background.
Bars = 50 μm; **(B)** to **(K)** have same scale bar as in **(C)**. Fifteen independent T1 GUS-positive, 3-d-old, light-grown seedlings were analyzed. Further expression analysis in lateral roots was performed with four independent T2 lines.

NDL Proteins Are Positive Regulators of Primary Root Length and Lateral Root Formation, and AGB1 Negatively Regulates NDL1 Mediation of Root Growth

Two independent transcript-null alleles for *NDL1*, *ndl1-1*, and *ndl1-2* were isolated from a T-DNA insertion population (see Supplemental Figures 5A and 5B online). Single *ndl1* loss-of-function mutants (*ndl1-1* and *ndl1-2*) did not display gross developmental defects (see Supplemental Figure 5C online). However, the loss-of-function mutant (*ndl1-2*) had a slightly shorter primary root length with wild-type lateral root density (Figures 5A and 5B). Since *NDL1* has two highly similar homologs, we sought available T-DNA insertion alleles for *NDL2* and *NDL3* from public resources but determined that these were not transcript-null alleles. Therefore, reduced expression of the entire *NDL* gene family was accomplished using two sets of microRNAs (miRNAs) that independently target the three *NDL* members (see Supplemental Figure 6 online for miRNA design; see Figure 5D for *NDL* mRNA levels). Hereafter, for simplicity, these *NDL*-reduced lines will be referred to as *ndlM1* and *ndlM2*. At least six transgenic lines transformed from each of these two miRNA targets showed similar phenotypes, and two were chosen for further characterization. The length of *agb1-2* primary roots was 2.9-fold greater than wild-type roots, while the root length of the *ndlM1* and *ndlM2* lines was slightly, yet statistically significantly, less than wild-type roots (Figure 5A). Primary root growth was somewhat compromised in the *ndlM1/M2* lines. Lateral root density was less for the single *ndl1-2* null mutant than for the wild type, although this reduction was not supported statistically. However, in lines with reduced expression of all three NDL homologs, lateral root density was reduced at least 2.7-fold ($P < 0.005$). This effect is in contrast with the *agb1-2* mutants, which showed a 1.4-fold increase compared with the wild type (Figure 5B; Chen et al., 2006a). For both primary root length and the lateral root density phenotypes, the *agb1-2* allele is possibly additive to the *ndl1-2* allele and to *ndl*M2 (cf. *agb1-2*, *ndl*M2, and *ndl*M2 *agb1-2* in Figures 5A and 5B). Overexpression of *NDL1* by the native *NDL1* promoter in wild-type roots resulted in increased primary root length with no significant effect on lateral root density (Figures 5A and 5B).

Auxin-induced lateral root formation was also determined. Reduction of *NDL* expression in Columbia-0 (Col-0) decreased the number of lateral roots 1.4-fold compared with the wild-type control, whereas *agb1-2* mutants showed an increase of 1.5-fold (Figure 5C, compare open and closed bars), consistent with previous findings by Ullah et al. (2003). Reduction of *NDL* gene expression in the *agb1-2* mutant *(agb1-2 ndlM2)* slightly diminished auxin induction of lateral root formation (Figure 5C, 1.2-fold compared with >1.5-fold for *agb1-2*).

AGB1 was shown to be a negative regulator of lateral root formation (Ullah et al., 2003), and our data indicate that NDL proteins act redundantly as positive effectors of root growth and

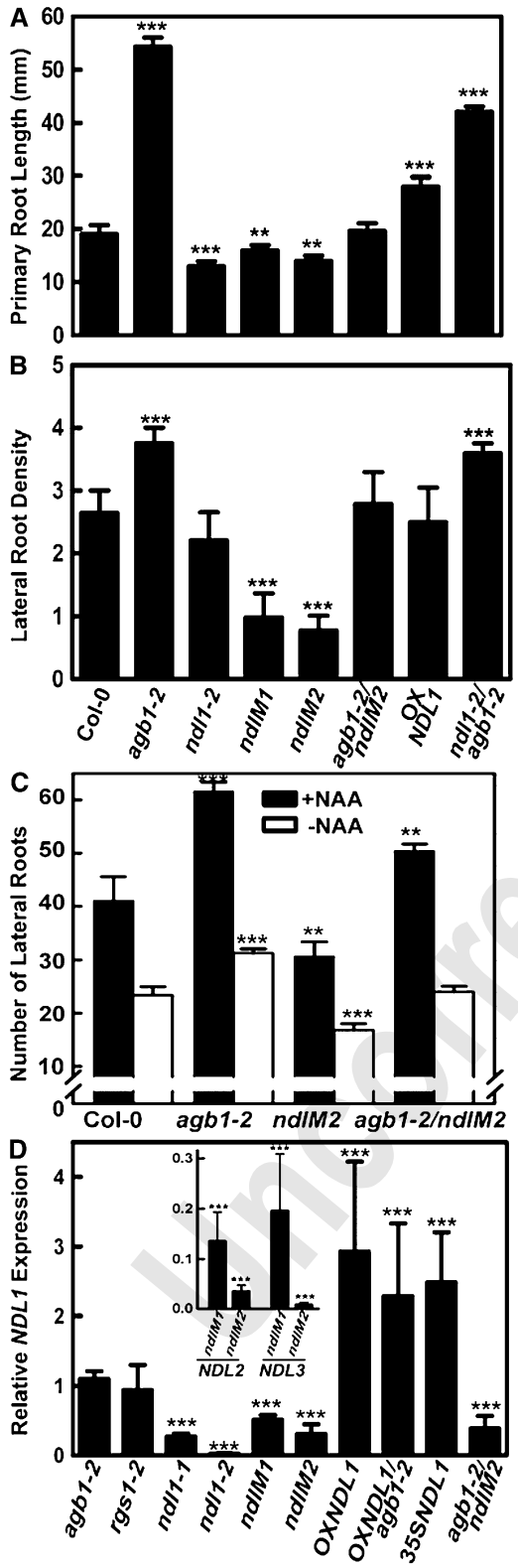

Figure 5. Effect on Root Length and Lateral Root Density by Altering *NDL* Levels in the Presence and Absence of *AGB1*.

lateral root formation (Figures 5A and 5B). Epistasis analysis suggests that NDL proteins and AGB1 have independent actions. However, since AGB1 and NDL proteins physically interact and since the stability of NDL1 in the root requires AGB1 (Figure 4), we favor an alternative possibility that is also consistent with the genetic data, namely, that AGB1 and NDL proteins operate together, albeit in parallel, in the same signaling pathway. Such network architecture often contains homeostatic loops that regulate the activity or stability of protein pairs (Yeger-Lotem et al., 2004).

G Protein Subunits and NDL Proteins Regulate Auxin Transport

The formation of lateral roots is regulated by auxin (Casimiro et al., 2001; Laskowski et al., 2006; De Smet et al., 2007; Fukaki et al., 2007). Gradients of auxin in the root are established by the concerted action of (1) various auxin transporters that transport auxin both basipetally and acropetally, (2) auxin synthesis at the root tip, and (3) degradation/deactivation at other positions of the root. Basipetal and acropetal streams of auxin transport are required for lateral root initiation and emergence phases, respectively (Casimiro et al., 2001). We previously reported that *agb1* (Ullah et al., 2003) and *agg* (Trusov et al., 2007) mutants have more lateral roots than the wild type, and we report here that *ndl* mutants have fewer lateral roots (Figure 5B).

Therefore, we hypothesized that mutations in *AGB1* and/or its partner Gγ subunits as well as mutations in *NDL* confer changes in auxin transport and consequently the auxin gradient in roots. To test this hypothesis, we examined basipetal and acropetal auxin transport in roots of various NDL and G protein mutant backgrounds (Figures 6A and 6B).

The *agb1-2* single mutant and the a*gb1-2 gpa1-4* and *agg1-1 agg2-1* double mutants displayed increased basipetal auxin transport compared with the wild type. The single *gpa1-4* and *rgs1-2* mutants had basipetal auxin transport rates that were close to the wild type level. The *agg1*-1 mutant showed increased while *agg2-1* mutants displayed reduced basipetal auxin transport compared with the wild type (Figure 6A). *ndl1-1* and *ndl1-2* both showed a decrease in relative transport, while *ndlM1* and *M2* lines also showed a decrease, corresponding with the decreased number of lateral roots. Both ectopic (35S) and

All experiments were repeated three times using 10 to 15 seedlings for each genotype in each trial.

(A) Root length (mm) of 9- to 10-d-old, short-day-grown seedlings (8:16, light:dark). The genotypes (described in the text) are indicated below **(B)**.

(B) Lateral root density (primordia and emergent roots per centimeter of primary root length) for roots described in **(A)**.

(C) Number of lateral roots with (black bars) and without (open bars) induction by 0.1 μM NAA.

(D) mRNA quantification of all the genotypes used was performed by qRT-PCR using gene-specific primers for *NDL1*, normalized to the *ACTIN2* transcript level. Expression level of *NDL2* and *NDL3* in *ndlM1* and *ndlM2* lines is shown as an inset. Error bars represent SE. Student's *t* test results are based on differences between the wild type and the indicated genotype shown as asterisks: **, $P < 0.05$; ***, $P < 0.005$.

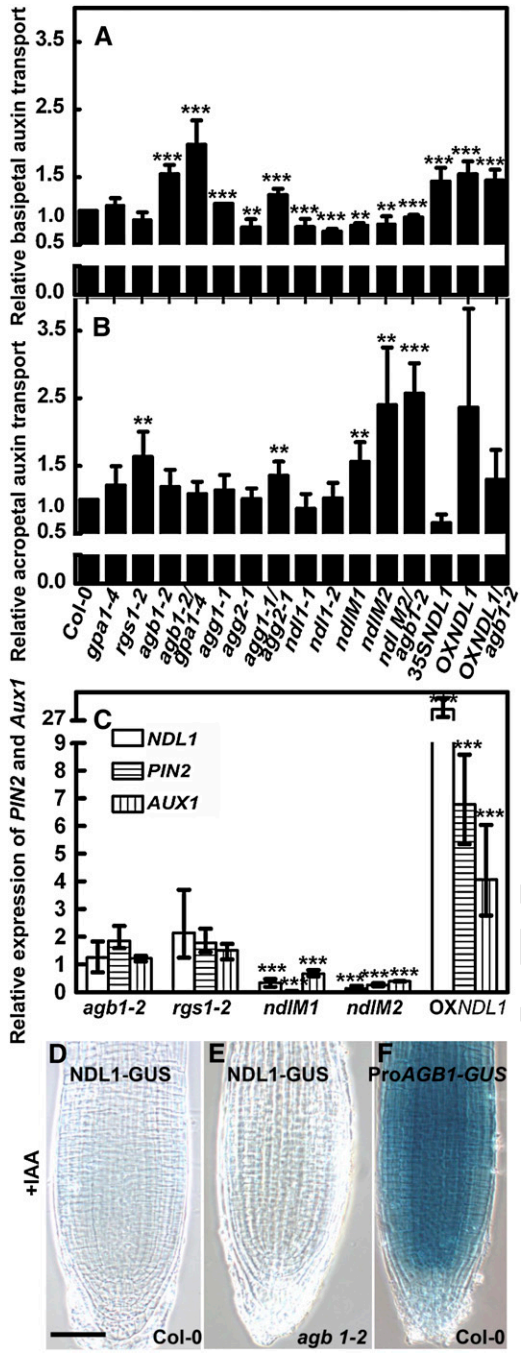

Figure 6. Relative Auxin Transport and Expression Level of *PIN2* and *AUX1* in Various G protein and *NDL* Genotypes.

(A) Basipetal auxin transport measured by applying [^{3}H]-IAA to the root apex and root-shoot junction as described in Methods.

(B) Acropetal transport measured as described in Methods. For both basipetal and acropetal transport, means ± SE are shown. The means are based on at least five independent trials, each involving >10 roots per genotype. Student's *t* test analysis based on differences between the wild type and the indicated genotype are indicated by asterisks above the bars: ***, $P < 0.001$; **, $P < 0.05$.

(C) qRT-PCR showing relative expression levels of *PIN2* and *AUX1* upon downregulation and overexpression of *NDL1* and in *agb1-2* and *rgs1-2* mutants. Data represent means ± SE of three replicates; similar results were obtained in three independent biological replicates. Student's *t* analysis based on differences between the wild type and the indicated genotypes are indicated by asterisks above the bars: ***, $P < 0.0001$.

(D) to **(F)** Effect of auxin application on NDL1 protein levels in the wild type **(D)** and *agb1-2* background **(E)** and on *AGB1* expression levels **(F)**. NDL1-GUS translational fusion and Pro*AGB1-GUS* lines were treated with 1 μM IAA, for 12 to 14 h, followed by GUS staining. Auxin decreased NDL1 steady state level and auxin increased *AGB1* expression compared with the untreated controls (c.f. Figures 4B, 4E, and 4H). Bar = 50 μm; each panel is equivalent in magnification.

native (OX) overexpression of *NDL1* resulted in increased basipetal auxin transport. Loss of AGB1 had no effect on this increased auxin transport conferred by native overexpression of *NDL1*, suggesting that *NDL1* acts downstream of or in parallel to *AGB1*. Reduced expression of all three *NDL* genes in *agb1-2* reduces (1.1-fold) the transport level toward wild-type levels (Figure 6A). Basipetal auxin transport directly correlated with the number of lateral roots. These results suggest that G protein and NDL family members regulate lateral root formation by affecting basipetal auxin transport.

Since both basipetal and acropetal auxin transport are responsible for changing local auxin gradients required to initiate lateral root formation, we also measured acropetal auxin transport in various genotypes. A significant and reproducible increase in acropetal transport was found in *rgs1-2*, in the *agg1-1 agg2-1* double mutant, and in the *NDL* reduced lines both with and without AGB1 (Figure 6B). Overexpression of *NDL1* showed the wild-type level of acropetal transport, indicating NDL proteins negatively affect acropetal auxin transport up to a threshold point. These findings suggest NDL proteins also regulate acropetal auxin transport and hence lateral root emergence as well as initiation.

These findings are in accordance with the pattern of NDL protein localization in the various regions and layers of the root. In the distal elongation zone of the root, NDL1 is localized in all the cell layers. Importantly, NDL1 is in the stele at a position that is higher than the root hair zone in the root (see Supplemental Figure 3G online), the site of acropetal auxin transport. NDL1 is localized in the initial stages of primordium formation (Figures 2P to 2S). The G protein complex components RGS1, AGB1, AGG1, and AGG2 also have a specific pattern of protein localization in various regions of the root. In response to a signal, NDL proteins could be free or bound to the components of the G protein core to regulate basipetal and acropetal auxin transport.

NDL Proteins Positively Regulate the Auxin Carrier *PIN2* and *AUX1* Expression, and Auxin Negatively Regulates NDL1 Localization around the RAM

Previously, we showed that AGB1 acts as a negative regulator of auxin-induced cell division, especially during formation of adventitious and lateral root primordia (Chen et al., 2006a). AGB1 acts directly or indirectly to repress basal expression of 25% of the auxin-inducible genes in seedlings, including key genes

necessary for lateral root formation (Ullah et al., 2003). NDL1 is a positive regulator of lateral root formation in the AGB1-mediated pathway. Because auxin transport rates are perturbed in NDL mutants and overexpression lines (Figures 6A and 6B), we determined the expression level of genes encoding the auxin efflux regulator PIN2 and the auxin permease AUX1 in *NDL* down- and upregulated lines. The steady state levels of *PIN2* and *AUX1* mRNA were significantly higher when *NDL1* was overexpressed (sevenfold and fourfold, respectively). In *ndl*M1 and *ndl*M2 lines, *PIN2* and *AUX1* mRNA levels were significantly reduced. In *agb1-2* and *rgs1-2* mutants, *NDL1* mRNA levels were not significantly different from wild-type levels (Figure 6C).

Several observations led us to hypothesize that AGB1, NDL1, and auxin operate in a feedback loop: (1) auxin transport streams are oppositely affected in *agb1*-null versus *ndlM1* and *ndlM2* lines (Figure 6), (2) NDL1 stability in the RAM requires AGB1 (Figure 4), (3) a pulse of auxin alters *AGB1* mRNA level (Ullah et al., 2003), and (4) lateral and primary root growth are oppositely affected in the respective loss-of-function lines (Figure 5).

NDL1-GUS translational fusion lines in wild-type Col-0 and the *agb1-2* background were treated with 1 μM indole-3-acetic acid (IAA) for 14 h, and GUS staining patterns of auxin-treated and untreated roots were compared (three independent lines were tested). Results of one representative line are shown. IAA treatment resulted in decreased NDL1-GUS staining in the wild type and no effect in the *agb1-2* background (Figures 6D and 6E) compared with untreated basal levels (Figures 4B and 4H; part of the same experiment). IAA increased *AGB1* expression (cf. Figures 4E and 6F; see Supplemental Figure 7 online). *ndl1-2* and *agb1-2* mutants have the opposite auxin response root phenotype. This indicates that auxin treatment has a negative effect on NDL1 protein stability and a positive effect on *AGB1* expression in the RAM, implicating both auxin-regulated, negative, and positive feedback loops in the RAM. Note that our results showing auxin-induced increase in *AGB1* mRNA appear to be in contrast with the results of Ullah et al. (2003), where it was reported that auxin causes a decrease in *AGB1* transcript level. This difference may be due to different auxin exposure times used in the two studies. The previous work examined a short-pulsed application of auxin. That study also did not account for differences in *AGB1* mRNA levels at the cellular level since whole seedlings were used. However, to mimic the expected chronic change in auxin levels caused by the observed difference in auxin transport, we treated roots with auxin over an extended time and then visualized the localization in the root tip, a site of high steady state level of NDL1 and of *AGB1* expression.

NDL Proteins Are Involved in Establishing Auxin Maxima and/or Auxin-Induced Gene Expression

Because *ndl* mutants have a small but significant decrease in basipetal auxin transport and have enhanced acropetal transport (Figure 6A), we hypothesized that NDL proteins play a role in setting up local auxin gradients in the root and therefore modulate expression of auxin-responsive genes. We used the auxin reporter *DR5-GUS* line to examine indirectly the location of auxin maxima in roots (Ulmasov et al., 1997). In the wild type, auxin maxima were observed at lateral root primordia (Figures 7A, arrows, and 7B to 7D); however, loss of NDL abolishes this pattern (cf. Figures 7E and 7F). This change in the auxin gradient and the formation of lateral root primordia is consistent with the observed NDL regulation of auxin transport (cf. Figures 6A and 6B; i.e., a positive effect on basipetal transport and a negative effect on the acropetal transport stream). The observed auxin at the root tip (Figure 7F) is likely due to auxin synthesized there or transported in the acropetal stream.

In the wild-type background, *DR5-GUS* expression increased throughout the root with exogenous auxin application (0.1 μM IAA, 14 h; Figures 7G to 7J). Notably, the tip region showed the maximum induction (Figure 7J). In the *ndl*M2 lines, the induction maxima were attenuated at the root tip (Figure 7G versus 7K); however, in the rest of the root, *DR5-GUS* expression was greatly attenuated (Figures 7K to 7N). Fifteen T1 independent lines were tested, and all roots showed the same pattern or in some cases, the expression level was lower throughout the root than the wild-type *DR5-GUS* expression. This suggests that exogenously applied auxin requires transport to achieve its effect since auxin transport is compromised in the *ndl*M1 and *ndl*M2 lines. Alternatively, NDL proteins may also regulate auxin sensitivity.

Since we observed significant differences between wild-type and *ndl*M1 and *ndl*M2 lines in lateral root phenotypes, changes in auxin transport, and changes in responsiveness of *DR5-GUS*, we conclude that *ndl* phenotypes are caused by defects in auxin transport and possibly also in auxin signaling.

Sucrose and D-Glucose Induce NDL1 Steady State Protein Levels

RGS1-coupled, G protein signaling plays an important role in sugar signaling in *Arabidopsis* (Chen et al., 2003; Chen and Jones, 2004; Johnston et al., 2007; Grigston et al., 2008). Since NDL1 is a physical interactor of AGB1/AGG and RGS1, and since RGS1 is a candidate sugar receptor, we tested the NDL1 steady state levels in response to various sugars. NDL1-GUS translational fusion lines in wild-type Col-0 and the *agb1* backgrounds were treated with various sugars, and the GUS pattern was examined to determine indirectly the effect of sugar on NDL protein steady state levels. Various concentrations of sugars (sucrose, D-glucose, L-glucose, sorbitol, glucuronate, and gluconate) ranging from 0 to 300 mM were applied to light-grown seedlings for various time intervals (see Supplemental Figure 8 online). Light increases the steady state level of NDL1 even in the absence of sugar treatment probably because of sugar synthesized by photosynthesis (see Supplemental Figure 8 online); consequently, sugar treatment in light-grown seedlings had higher basal levels of GUS staining compared with dark-grown seedlings (cf. no sugar treatment in Supplemental Figure 8 to Figure 8G).

Dark-grown seedlings were used for sugar treatments in order to observe a larger induction difference. Treatment with sugar (100 mM, ~2%) for 8 h was optimal and was used in further experiments. We found that sucrose and D-glucose increased the NDL1-GUS activity, which was higher (Figures 8A and 8B) than in control plants (Figure 8G). Sorbitol and L-glucose treatment showed no induction of GUS activity (Figures 8H and 8I), indicating the effect was stereospecific and not due to osmotic

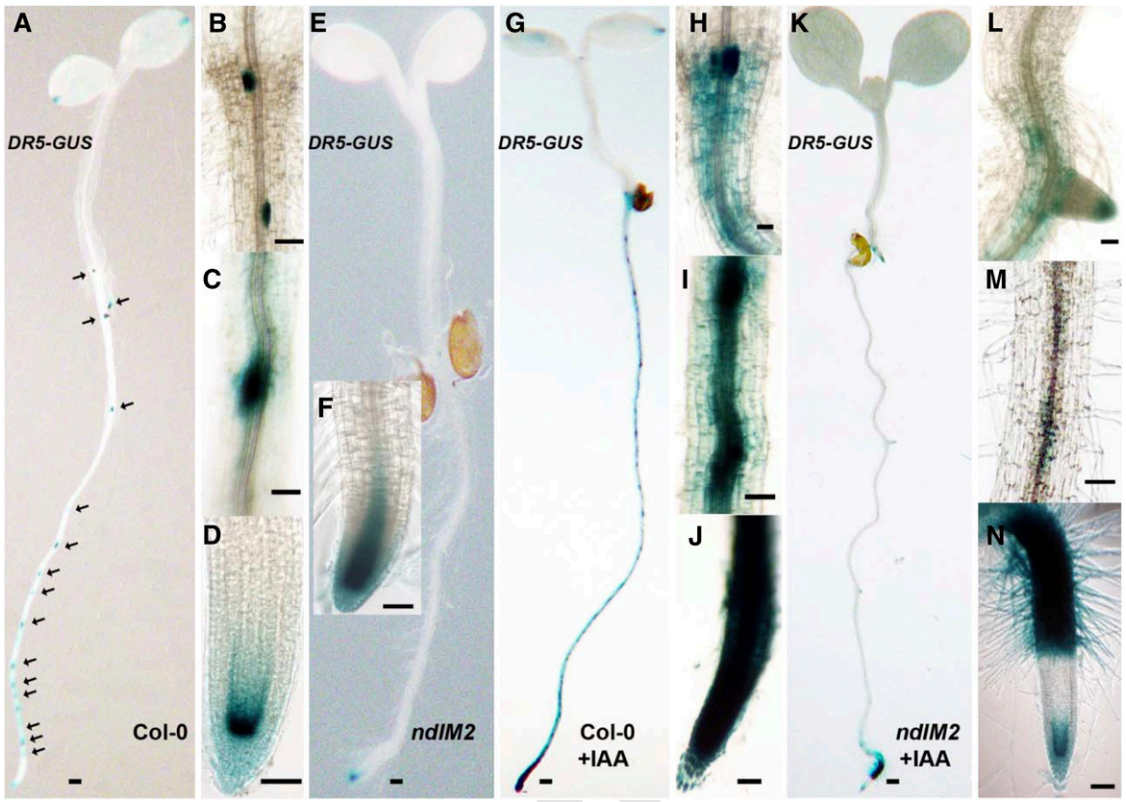

Figure 7. Auxin Maxima in the Wild Type and in Lines with Reduced Expression of *NDL* Genes.

(A) to **(D)** Spatial pattern of the auxin reporter, *DR5-GUS*, in the wild-type background. Black arrows indicate lateral root primordia.
(B) to **(D)** Higher magnification of auxin maxima observed at the apical meristem **(B)**, root **(C)**, and root tip **(D)**.
(E) *DR5-GUS* pattern in lines with reduced expression of the *NDL* gene family using miRNA in the reporter background. Loss of NDL proteins decreased the number and intensity of auxin maxima.
(F) Detailed view of the tip still showing deep staining pattern in **(E)**.
(G) *DR5-GUS* in the wild-type background treated with 0.1 μM IAA for 14 h.
(H) to **(J)** As for **(B)** to **(D)** except for the root shown in **(G)**.
(K) *DR5-GUS* expression patterns in the silenced *NDL* background with IAA induction.
(L) to **(N)** As for **(B)** to **(D)** except of the root shown in **(K)**.
Genotypes are indicated. Bars = 50 μm.

stress. *AGB1* expression also increased upon D-glucose and sucrose treatment (Figures 8C and 8D) compared with the untreated control (Figure 4E). In the absence of AGB1, sugars were able to restore NDL1 levels closer to the wild-type, untreated levels (Figures 8E and 8F for untreated controls; see Figure 8G for dark-grown and Figure 4B for light-grown levels). This suggests interplay of sugar and AGB1 in regulating the steady state NDL1 levels in roots.

Sugars Increase Lateral Root Formation and the Auxin Gradient in the Root Tip

Because NDL1 protein showed increased steady state levels in response to sucrose and D-glucose, we tested the response of these two sugars on lateral root formation in various *NDL* downregulated and upregulated backgrounds. Exogenous sucrose and D-glucose increased the number of lateral roots in all genotypes tested (the wild type, *agb1-2*, *rgs1-2*, *ndl*, and *NDL1*OX) compared with the respective no-sugar controls (Figure 8J). Consistent with *rgs1* hyposensitivity to sugars, D-glucose was less effective at stimulating lateral root formation in the *rgs1-2* mutant. Both sucrose and D-glucose stimulated lateral root formation in *agb1-2* compared with the wild type. In the absence of NDL proteins, fewer lateral roots formed. Overexpression of *NDL1* increased the number of lateral roots even in the absence of sugars. Sucrose, but not D-glucose, had an additional stimulatory effect.

Compared with the control, the number of sugar-induced lateral roots was reduced significantly upon naphthylphthalamic acid (NPA) treatment for all the genotypes other than *agb1-2* (Figure 8K). *agb1-2* was hyposensitive to NPA treatment in the absence of sugars, confirming findings by Pandey et al. (2008). In the presence of sugars, the effect of NPA was less for *agb1-2* compared with other genotypes (other than *ndlM2*), which

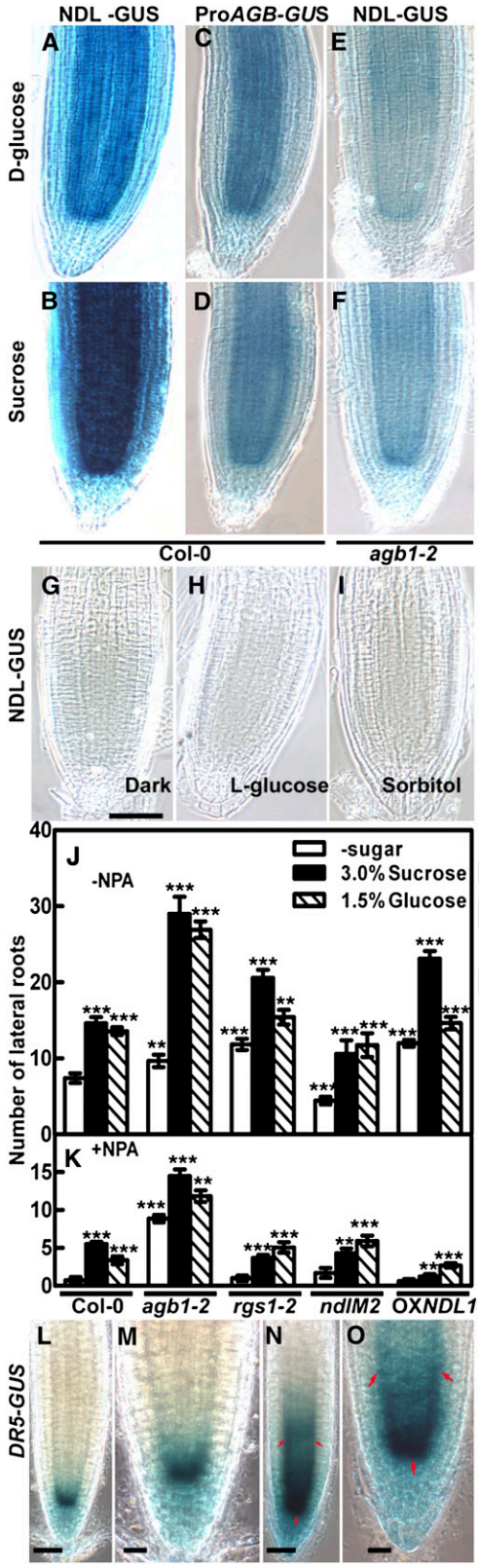

Figure 8. Steady State Levels of NDL1-GUS and *AGB1* Expression in Response to Various Sugar Treatments in the Presence and Absence of AGB1.

showed a similar sensitivity to NPA as the wild type. These results suggest that sugar stabilizes the steady state levels of NDL proteins. In this scenario, the increase in NDL1, and hence the sugar effect on lateral root formation, is mediated by auxin transport.

In order to test this hypothesis, we used the auxin reporter *DR5-GUS* line to examine the effect of sugar on local auxin gradients. Three-day-old, dark-grown seedlings were treated with 300 mM sucrose and compared with the untreated control after 12 h. In untreated seedlings, local auxin maxima are confined to the meristem (Figures 8L and 8M). Upon sugar treatment, the auxin gradient spreads to the layers above and below the meristem (Figures 8N and 8O, compare position of red arrows). This indicates that sugar has a positive effect on the free auxin gradient and transport at the root tip. A recent report also showed that in wild-type roots, basipetal auxin transport increases with increasing glucose concentrations (Mishra et al., 2009).

DISCUSSION

We propose a novel signaling cassette minimally comprised of RGS1, the heterotrimeric G protein complex subunits (GPA1, AGB1, and AGG), and NDL1. Putative NDL orthologs (NDR proteins) were previously reported from animals as well as from plants, but their function was unclear. We provide evidence that they are members of the Gβγ signaling pathway in plants and speculate that this is true for animal cells.

(A) to **(F)** Five-day-old dark-grown seedlings were treated with 100 mM sucrose or D-glucose for 8 h, followed by X-gluc staining. The optimal time and dose was predetermined for NDL-GUS (see Supplemental Figure 8 online).
(A) and **(B)** NDL-GUS level in response to D-glucose **(A)** or sucrose **(B)**.
(C) and **(D)** Pro*AGB1-GUS* expression in response to D-glucose **(C)** or sucrose **(D)**.
(E) and **(F)** NDL steady state levels in the *agb1-2* background in the presence of D-glucose **(E)** or sucrose **(F)**.
(G) to **(I)** Control, dark-grown seedlings on NDL-GUS seedlings on half-strength MS medium without sugars **(G)**, with L-glucose **(H)**, and with sorbitol **(I)**. These controls showed no staining for NDL-GUS. For the untreated control of Pro*AGB-GUS* and *agb1-2*, see Figures 4E and 4H, respectively. **(A)** to **(I)** have same scale bar as in **(G)**.
(J) and **(K)** Sugar-induced lateral root formation in the absence **(J)** and presence **(K)** of NPA in various G protein and *NDL* genotypes. Student's *t* test analysis based on differences between sugar treatment of the wild type and the indicated genotypes are indicated by asterisks above the SE: ***, $P < 0.001$; **, $P < 0.05$. Sugar treatments are compared to control in the wild type or controls among all genotypes. These experiments were repeated three times, and the same pattern of lateral root formation was observed. For each experiment, 15 to 20 seedlings were counted.
(K) Same as **(J)** except 5 μM NPA was included.
(L) to **(O)** Three-day-old, dark-grown seedlings were treated with 300 mM sucrose for 12 h (**[N]** and **[O]**) and compared with the untreated control (**[L]** and **[M]**). Red arrows indicate increased areas of GUS staining. **(M)** and **(O)** represent high magnification of **(L)** and **(N)**, respectively. Bars = 50 μm.

Indirect evidence from work with animal cell lines supports a possible role for these genes in cell proliferation and/or differentiation. *NDR1* expression is repressed by proto-oncogenes N-myc and C-myc in embryonic cells and in proliferating tumors cells (van Belzen et al., 1998; Shimono et al., 1999). *NDR1* expression is upregulated by tunicamycin, calcium ionophore, hypoxia (Salnikow et al., 2000; Lachat et al., 2002), and at G1/G2 stages of the cell cycle (Kurdistani et al., 1998; Piquemal et al., 1999; Guan et al., 2000). In mast cells, NDR1 is phosphorylated and interacts with HSP70 (Sugiki et al., 2004a, 2004b). NDR1 proteins are members of the lipase/esterase superfamily containing an α/β hydrolase fold and fall specifically within a subfamily that lacks the canonical catalytic triad (Shaw et al., 2002). The precise molecular and cellular function of NDR proteins is unknown, but one NDR protein, NDRG1, is a novel effector for the small GTPase, Rab4a, and is important in recycling E-cadherin in proliferating cells (Kachhap et al., 2007). *NDR* genes were isolated by mRNA differential display between differentiated and proliferating tumor cells (e.g., human myelomonocytic U937 cells and human mammary carcinoma MCF-7 cells). The human *NDR1* gene is downregulated in tumor cells and upregulated in differentiated cells that cease to proliferate. The hypothesized functions for NDR1 include a role in cell growth arrest and terminal differentiation (van Belzen et al., 1998; Piquemal et al., 1999; Guan et al., 2000). We speculate that while it is possible that NDL/NDR protein functions in plants and animal cells manifest differently, their function in a G protein pathway is the same. For example, a possible function of NDR proteins in animal cells is to attenuate cell proliferation, while *Arabidopsis* NDL1 promotes cell proliferation, specifically of pericycle cells, leading to the formation of lateral roots. Both cell proliferation and lateral root formation involve Gβγ (Dhanasekaran et al., 1998; van Belzen et al., 1998; Shimono et al., 1999; Ullah et al., 2001; Chen et al., 2003). Our previous work established that AGB1 acts as a negative regulator of auxin-induced cell division in lateral root formation and speculated that AGB1 blocks reentry into the cell cycle (Ullah et al., 2003; Chen et al., 2006a). Gene expression profiles of wild-type and *agb1-2* seedlings upon IAA treatment showed that a set of auxin-regulated genes are derepressed in the *agb1-2* background. One of these is *LATERAL ROOT PRIMORDIA*, a gene essential for lateral root formation (Smith and Fedoroff, 1995). Previously, it was shown that auxin-induced cell division does not strictly require a G protein for direct coupling but rather that the sensitivity toward auxin is attenuated by G proteins (Ullah et al., 2003). Trusov et al. (2007) showed that AGB1/AGG1 is expressed in the central vascular cylinder, while AGB1/AGG2 is expressed in the cortex and epidermis. They hypothesized that AGB1/AGG1 and AGB1/AGG2 regulate acropetal and basipetal auxin transport, respectively, within their respective tissues (Trusov et al., 2007). Although the role of G protein components has been well established in lateral root formation, the mechanism by which they act was previously unknown. Here, we report altered auxin transport in various G protein mutants as well as in various *NDL1* genetic backgrounds. We conclude that NDL1 is a component of G protein signaling and is a positive regulator of primary root length and lateral root formation. It is well established that auxin transport promotes lateral root initiation and plays an important role in root growth (Casimiro et al., 2001; Grieneisen et al., 2007). We show that G protein components and NDL1 act on basipetal and acropetal auxin transport to regulate lateral root formation.

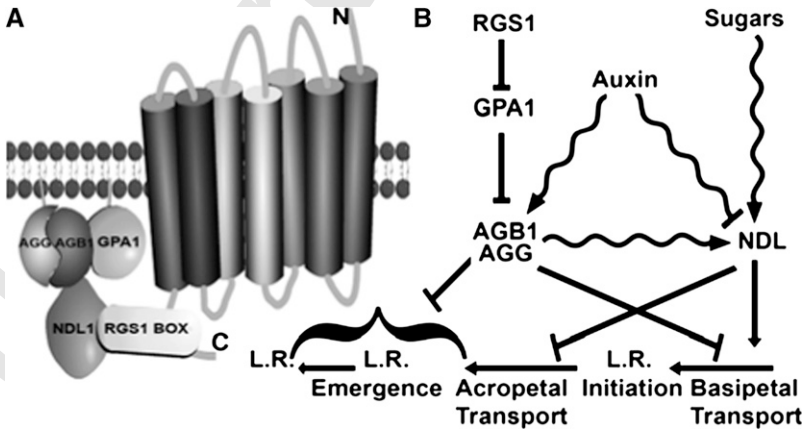

Figure 9. Proposed Physical Relationship of NDL in the G Protein Complex and a Model of the Mode of Action of NDL.

(A) Physical interaction model. NDL1 is shown as part of the G protein–coupled pathway on the membrane. Interactions that have been shown here are between the AGB1 and RGS1 with NDL proteins. Previous work described in the text supports interactions between RGS1 and GPA1 and between GPA1 and AGB1 in *Arabidopsis*.

(B) Genetic and biochemical interaction model. Epistasis analysis predicts that AGB1 and NDL proteins act, at least in part, via independent parallel pathways. The genetic data are also consistent with AGB1 and NDL1 acting in a complex where NDL1 is a positive and AGB1 is a negative regulator of lateral root formation, but the mechanism is unclear as represented by the bracket. NDL1 and AGB1 regulate auxin-induced lateral root formation via their effect on auxin transport. NDL1 promotes the flux of the basipetal stream of auxin transport and hence on lateral root initiation. AGB1 has the opposite action. AGB1, sugars, and auxin operate on NDL in the feedback loops indicated by the wavy lines. The scheme does not illustrate the redundant nature of the three NDL proteins. L.R., lateral root.

Mature *Arabidopsis* roots are self-sufficient in auxin biosynthesis with auxin maxima existing in the quiescent center (Grieneisen et al., 2007; Petersson et al., 2009). Local auxin biosynthesis and transport establishes and maintains the auxin gradient in the root, which in turn instructs lateral root initiation (in a zone basal to the RAM) (Dubrovsky et al., 2000; Grieneisen et al., 2007; Petersson et al., 2009) and emergence phases (Casimiro et al., 2001; Bhalerao, et al., 2002). We found that the localization pattern of NDL1 protein at the root apex (Figures 2B and 2N; see Supplemental Figure 3F online), for the most part, coincides with the auxin maxima in the root. We show that the stability of NDL1 at the primary and lateral root meristem is positively regulated by sugar and AGB1, whereas it is negatively regulated by a high concentration of auxin (1 μM). By contrast, long-term exposure of auxin has a positive effect on *AGB1* expression. We propose that this posttranslational regulation of NDL1 by auxin, sugars, and AGB1 is required to maintain the optimal NDL concentration, to achieve normal basipetal and acropetal auxin transport needed to regulate lateral root initiation and emergence, and to define the zone of lateral root formation in the root. These findings indicate a highly regulated network of positive and negative feedback loops to fine-tune auxin transport.

Putative NDR orthologs had not been studied previously in a eukaryotic multicellular context or linked to the G protein pathway. For plants, the AGB1/NDL complex indirectly modulates expression of auxin transport components, such as the PIN2 proteins and AUX1 (Friml et al., 2002; Benjamins et al., 2005; Geisler et al., 2005; Wisniewska et al., 2006; Grieneisen et al., 2007; Zazimalova et al., 2007; Bainbridge et al., 2008; Benjamins and Scheres, 2008). While the biochemical function of NDL proteins is unknown, the similarity of NDL1 to lipases permits us to speculate that NDL1 alters membrane composition resulting in altered PIN protein activity or location.

Disruption of auxin influx carrier proteins also results in abnormal phyllotaxis and clusters of primordia and reduced auxin maxima and coordinated PIN polarization (Bainbridge et al., 2008). Auxin patterns established by polar auxin transport are also critical throughout plant development, and AGB1 is also known to regulate or couple signaling pathways in organs beyond the root. This begs the question of a possible role for NDL in aerial tissue development. A preliminary answer comes from characterization of the loss-of-*NDL*-function lines. Reducing NDL protein levels confers a number of aerial phenotypes that likely result from an altered auxin economy or distribution pattern.

In *Arabidopsis*, high concentrations of exogenous auxin trigger nearly all of the pericycle cells adjacent to protoxylem poles to divide to form lateral root primordia (Himanen et al., 2002). Overexpression of auxin biosynthesis genes also produces more lateral roots. In addition, inhibition of polar auxin transport from its site of synthesis in the upper parts of the plant to the root also inhibits the formation of lateral roots. One view is that deprivation of auxin keeps pericycle cells in the G1 phase, while readdition of auxin promotes the G1/S transition (Stals and Inze, 2001). Various cell cycle regulators like cyclin D, cyclin-dependent kinase, and its inhibitor KRP2 are also implicated in lateral root initiation (Casimiro et al., 2003). In our search for NDL1-interacting proteins through yeast three-hybrid screens, we found CYCLIN-DEPENDENT REGULATORY SUBUNIT2 (AT2G27970) as a candidate interacting partner, suggesting NDL1 acts at the cell cycle level in the process of lateral root formation.

Interplay of auxin and sugars in induction and differentiation of the vasculature has been known since the 1950s, but the molecular mechanism and components involved in the pathway were not known. Classical experiments performed by Wetmore showed that auxin and sugars can lead to differentiation of vascular cells in callus of *Syringa* (Wetmore and Sorokin, 1955). A specific ratio of auxin and sugars is required for the induction and complete differentiation of xylem and phloem in callus tissue of angiosperms (Wetmore and Rier, 1963). There are three mutants linking auxin and glucose signaling pathways: the glucose-insensitive mutant *gin2*, the turanose-insensitive *tin*, and *hls1* (Moore et al., 2003; Gonzali et al., 2005; Ohto et al., 2006). A report using whole-genome approaches in *Arabidopsis* described a glucose interaction with auxin signaling and transport to regulate root growth and development (Price et al., 2004). Mishra et al. (2009) concluded that the glucose effect on plant root growth and development is mediated by auxin signaling components.

Since we found that NDL1 interacts with AGB1 and RGS1, we propose that NDL1 acts as part of a multimeric protein complex to regulate auxin transport at the membrane. Current (Figures 1A and 1B) and previous data from our lab and other labs support the G protein component interactions shown in Figure 9A (e.g., Mason and Botella, 2001; Chen et al., 2003; Kato et al., 2004; Chen et al., 2006c; Fan, et al., 2008).

The scheme shown in Figure 9B summarizes the genetic (straight arrows) and biochemical (wavy arrows) interactions found in this study. Sugars (Figures 8A and 8B; see Supplemental Figure 8 online), AGB1 (Figures 4B and 4H), and light (Figures 4B and 8G; see Supplemental Figure 8 online) increase the steady state level of NDL1 protein acting as positive regulators of the pathway, whereas auxin has an inhibitory effect at higher concentrations (Figures 4B and 6D), indicating the existence of a negative feedback loop. *AGB1* expression is positively regulated by auxins (Figures 4E and 4F; see Supplemental Figure 7 online), which in turn have a positive effect on posttranslational stability of NDL1 (Figures 4H to 4K), indicating the existence of a positive-feedback loop of regulation. NDL proteins play an important role in establishing local auxin maxima or gradients (Figure 7) by regulating basipetal (Figure 6A) and acropetal (Figure 6B) auxin transport and thus modulate lateral root initiation and emergence (Figures 5A and 5B).

METHODS

Protein–Protein Interaction by Complementation Screening in Yeast

The coding sequence of *AGB1* was cloned into the pBridge vector (Clontech) as a DNA-BD fusion protein. *AGG1* or *AGG2* was cloned in the same plasmid driven by the *MET*25 promoter to provide Met repression (primers and restriction site information provided in Supplemental Table 1 online). Three cDNA expression libraries as prey activation domain fusions were interrogated. pACT2 was used as the plasmid backbone for

the libraries prepared using the Clontech Matchmaker cDNA Library kit (Clontech). Interactions were scored by growth on histidine and adenosine drop-out media as described and confirmed by expression of β-galactosidase enzyme. All media and reagents were made as indicated by the manufacturer (Clontech). To confirm the results of the screen, entry clones for all three *NDL* gene family members were created in the pENTR/D-TOPO vector (Invitrogen) and then recombined into the activation domain (AD)-containing and pBridge-compatible pACTGWattR GATEWAY vector (Nakayama et al., 2002). Yeast three-hybrid interactions were confirmed by transforming AH109 strain with pBridge containing *AGB1*/*AGG2* or *AGG1* and interactors in the pACTGWattR backbone.

Phylogenetics

A multiple-sequence alignment was generated with ClustalX (Thompson et al., 1997). The Gonnet series of matrices was used with gap opening and extension penalties of 10 and 0.2, respectively. For the phylogenetic analysis, the alignment was manually adjusted with major gaps removed. The phylogenetic tree was calculated with MrBayes (Huelsenbeck et al., 2001; Ronquist and Huelsenbeck, 2003). The fixed equalin model with an inverse γ rate was used. A sampling frequency of 100 was used for three independent runs of 100,000 generations. All nodes had higher than an 80% credibility score.

Plant Material

The ecotype used here was Col-0. Mutations were generated by T-DNA insertion (*ndl1-1* and *ndl1-2*) or by the indicated RNA silencing constructs (ndl*M1* and *ndlM2*; see Supplemental Figure 6 online for primer design). *agg1-1*, *agg2-1* (Trusov et al., 2007), *agb1-2* (Ullah et al., 2003), and *rgs1-2* (Trusov et al., 2007) mutants have been previously described. *Arabidopsis thaliana* seeds were surface sterilized then stratified for 2 d. Seeds were sown on half-strength Murashige and Skoog (MS) plus 1% sucrose.

Cloning of *NDL* Gene Family Members and Derivative DNA Constructs and Expression

The *NDL1* mRNA obtained in the Y3H screen was full length. The NDL1 coding region was PCR amplified from the yeast clone. *NDL2* and *NDL3* cDNA was PCR amplified using first-strand *Arabidopsis* cDNA as template. All three genes were cloned into pENTR D/-TOPO (Invitrogen) and sequenced. Expression vectors were generated by recombination using GATEWAY technology (Invitrogen). Oligonucleotides used in this study are shown in Supplemental Table 1 online.

[AQ3] The *NDL1* cDNA was cloned into plasmid pGWB21 (N-myc), pK7FWG2 (N- and C-GFP), and pGWB45 (N-CFP). A genomic fragment of NDL1 containing both 780 bp of the 5′ promoter and the entire gene was cloned and recombined into pGWB3 (GUS), pGWB4 (GFP), pGWB40 (YFP), and pGWB43 (CFP). The *NDL1* promoter was cloned into pGWB3 (GUS) and pGWB4 (GFP) (Nakagawa et al., 2007). Designations of derivative plasmids are provided in Supplemental Table 2 online.

mRNA Quantification

RNA was isolated from various tissues using Trizol (Invitrogen). RT-PCR was performed using the ThermoScript RT-PCR system (Invitrogen). First-strand cDNA synthesis was performed using an oligo(dT) primer. RT-PCR reactions were performed using internal gene-specific primers. For qRT-PCR, first-strand cDNAs were synthesized as described for RT-PCR. qRT-PCR primers were designed using Beacon designer 7.5 software from Premier Biosoft International and GenScript real-time PCR (TaqMan) Primer Design (http://www.genscript.com/ssl-bin/app/primer). Fragments ranging from 98 to 133 bp for *NDL1*, *NDL2*, *NDL3*, *AUX1*, and *PIN2* were amplified (for GenBank accession numbers and primer sequences, see Supplemental Table 1 online) to quantify transcript levels. Fifty-microliter reactions for qRT-PCR contained 25 μL of SYBR GREEN PCR Master Mix (Applied Biosystems), 100 ng of cDNA from the first-strand cDNA synthesis reaction, and primers specific for the gene to be quantified or the reference gene (*ACTIN2*) at final concentrations of 0.2 pmol/μL. Reactions were performed in triplicate, and three biological replicates were done.

NDL1 Structure Modeling

The NDL1 protein sequence was submitted to the BioInfoBank Meta-Server (http://meta.bioinfo.pl) for protein fold recognition and template identification (Ginalski et al., 2003). The MetaServer obtains a consensus of results from fold recognition servers: 3D-PSSM, Fugue, Inub, Sam-T02, and mGenThreader. Five different homology models were built based on five different templates identified by the MetaServer. The models were built using the homology suite of Insight II (Accelrys), and the sequence structure compatibility of the generated atomic models was evaluated using Profiles-3D. The model with the highest score had the best fold and was selected as the final model.

Promoter and Genomic Fragment of *NDL1*

The *NDL1* gene was PCR amplified from 1000 bases upstream of the start codon to the last codon (plus or minus the stop codon as appropriate) using high-fidelity Phusion (Finnzymes). The resulting products were cloned into pENTR D-TOPO and verified to be error free.

Arabidopsis Plant Transformation

Binary vector constructs were mobilized into the *Agrobacterium tumefaciens* strain GV3101 by electroporation. *Arabidopsis* plants were transformed using the floral dip method (Clough and Bent, 1998). Transformed plants were selected on half-strength MS plus 1% sucrose growth medium containing the appropriate antibiotic selection.

GUS, Lipase-Esterase, and Lateral Root Assays

Histochemical GUS staining was performed as described by Malamy and Benfey (1997). All samples were gently degassed for 5 min. After staining overnight at 37°C, the samples were rinsed three times (37°C, 75% ethanol) and stored in 75% ethanol.

Lateral root assays were performed as described by Ullah et al. (2003). Briefly, lateral root density is calculated as the number of discernable primordia and emergent roots per centimeter of primary root length of 9- to 10-d-old seedlings grown on vertical plates (half-strength MS, 1% sucrose, and 0.75% agar, 22°C, 8:16 light:dark cycle). To assay for auxin-induced lateral root formation, seedlings were first grown horizontally for 9 d on 5 μM NPA (half-strength MS plus 1% sucrose) and transferred to vertical plates with or without 0.1 μM NAA for 5 d under continuous light. [AQ4] To assay sugar-induced lateral roots, seeds were plated on solid media (half-strength MS, 1% sucrose, and 0.75% phytoagar) with various concentrations of sugars with and without NPA (5 μM), and seedlings were vertically grown for 9 d (8:16 light:dark cycle). Lateral root number and primary root length were determined using light microscopy.

The *NDL1* coding region in pENTR D/-TOPO was recombined into the pDEST 17 vector, and poly- Histidine-tagged NLD1 protein was produced by expression in *Escherichia coli* strain BL21 (DE3)pLysS (Promega). Recombinant NDL1 was affinity purified using TALON resin according to the manufacturer's protocol (Clontech). Partially purified protein was obtained, and lipase-esterase assays were performed using

the Quantichrom lipase assay kit (Bio Assays Systems). Lipase-esterase activity was also tested using various ρ-nitro phenol esters of different alkyls as substrates (Yang et al., 2002).

IAA, NPA, and the indicated sugars were purchased from Sigma-Aldrich. IAA and NPA were purified further to >99% purity. Sugar stocks were prepared fresh.

Agrobacterium-Mediated Transient Expression and Coimmunoprecipitation in *Nicotiana benthamiana*

Cotransformation of *N. benthamiana* with *Agrobacterium* harboring plasmids expressing either an N-flag-AGB1 in pGWB12, N-CFP-NDL1 in pGWB45, or N-GST-NDL1 in pGWB22 was performed. After transient expression for 22 h, *N. benthamiana* leaves (0.3 g) were harvested and immunoprecipitations were performed (Day et al., 2006). Antibodies were obtained from the following manufacturers: anti-FLAG, Sigma-Aldrich; anti-GFP, Invitrogen; and anti-GST, Invitrogen. Protein A Sepharose was used (Pierce Biotech). Protein samples were analyzed by SDS-PAGE on 12% polyacrylamide gels (Laemmli, 1970) and transferred for immunoblot analysis by electrophoretic transfer to nitrocellulose membranes. Membranes were probed using anti-Flag, anti-GFP, and anti-GST primary antibodies.

Generation of miRNA Lines with Reduced *NDL* Gene Family Expression

Two common regions unique to three members of *Arabidopsis NDL* genes (5′-TAGCTCCTAACTCATGCCGAG-3′ and 5′-TCCATTCAGACCATGAAGGTG-3′) were selected, and miRNAs were designed using WMD2-Web MicroRNA Designer Web tool (http://wmd.weigelworld.org/cgi-bin/mirnatools.pl) except that primers A and B were replaced by Micro topo A and Micro topo B primers (see Supplemental Table 1 for sequence and Supplemental Figure 6 for primer design). Six T2 lines from each miRNA target set showing significant downregulation of *NDL1* were characterized. An important finding was that in the T3 generation, silencing by miRNA was lost.

Auxin Transport Assays

Basipetal and acropetal auxin transport measurements were performed in various genetic backgrounds as described by Lewis and Muday (2009). Seedlings were grown vertically under short-day conditions (8 h light and 16 h dark; 100 μmol m^{-2} s^{-1}) for 5 to 7 d on half-strength MS with 1% sucrose. Ten to fifteen seedlings were moved to a fresh plate and aligned at the root tip, and [^{3}H]-IAA agar lines (final concentration = 100 nM) were applied to the aligned root tips of the seedling for basipetal auxin transport assays. Plates were incubated vertically in the light chamber (100 μmol m^{-2} s^{-1}) for 5 h. Subsequently, the first 2 mm of the root tip touching the radioactive agar were discarded and the 5-mm section of the root above the site of cut was assayed for radioactivity by scintillation counting. For acropetal auxin transport assays, [^{3}H]-IAA agar lines (final concentration = 200 nM) were applied just below the root-shoot junction. Plates were wrapped with aluminum foil, inverted, and incubated vertically in the dark for 18 h. After incubation, agar lines were removed and 5-mm sections from the root tip were cut and assayed as described for basipetal transport.

Microscopy

Subcellular localization of NDL1-fluorescent protein fusions were performed using a Zeiss LSM510 confocal laser scanning microscope and Olympus XI81 inverted microscope platforms. Light microscopy was performed using a Nikon inverted microscope DIAPHOT-TMD. Root samples were cleared with a chlorohydrate solution (80%) before imaging. Cross and longitudinal sections of the GUS-stained roots were prepared using JB-4 plastic (Electron Microscopy Sciences) as described in John Schiefelbein lab protocols (http://www.mcdb.lsa.umich.edu/labs/schiefel/protocols.html). Sections of 10-μm thickness were cut using a triangular glass knife with a microtome (2065 Supercut Microtome), transferred to slides mounted with permount, and imaged.

Accession Numbers

Sequence data from this article can be found in the GenBank/EMBL data libraries under the following accession numbers: At4g34460 (*AGB1*), At3g63420 (*AGG1*), At3g22942 (*AGG2*), At3g26090 (*RGS1*), At5g56750 (*NDL1*), At5g11790 (*NDL2*), At2g19620 (*NDL3*), At3g18780 (*ACTIN2*), At5g57090 (*PIN2*), At2g38120 (*AUX1*), and BC071235 (NDRG1).

Supplemental Data

The following materials are available in the online version of this article.

Supplemental Figure 1. In Planta Protein Interaction of AGB1 and NDL1

Supplemental Figure 2. Clustal X Multiple Sequence Alignment of NDR Proteins from Various Organisms.

Supplemental Figure 3. Expression Analysis of *NDL1*.

Supplemental Figure 4. In Vivo Protein Levels of NDL1 Protein in Lateral Roots the Presence and Absence of *AGB1*.

Supplemental Figure 5. *ndl1* Genotype and Gross Phenotype.

Supplemental Figure 6. ClustalW Multiple Sequence Alignment of *NDL1.*

Supplemental Figure 7. Pro*AGB-GUS* Expression Pattern in Response to IAA.

Supplemental Figure 8. Steady State NDL1-GUS Protein after Treatment with Various Sugars.

Supplemental Table 1. Primers Used for the PCR Reactions.

Supplemental Table 2. Various *NDL* Constructs Generated during the Study

Supplemental Data Set 1. ClustalX Multiple Sequence Alignment of NDR Proteins from Various Organisms Used to the Generate Phylogentic Tree Presented in Figure 1C.

ACKNOWLEDGMENTS

This work was supported by the NIGMS (R01GM065989), the Department of Energy (DE-FG02-05er15671), and the National Science Foundation (MCB-0723515 and MCB -0718202) to A.M.J. and by the DFG to J.F.U. We thank Jing Yang and Cathy Jones for technical assistance and Mara Duncan for use of the plate reader in the lipase assays. We thank Tony Perdue for his technical support with the microscopy analyses. We thank Poornima Sukumar, Gloria Muday, and Zhongying Chen for their advice on how to perform the auxin transport assays and interpret the results.

Received January 12, 2009; revised October 8, 2009; accepted October 28, 2009; published ■■■.

[AQ5]

REFERENCES

Akgoz, M., Azpiazu, I., Kalyanaraman, V., and Gautam, N. (2002). Role of the G protein gamma subunit in beta gamma complex modulation of phospholipase Cβ function. J. Biol. Chem. **277:** 19573–19578.

Bainbridge, K., Guyomarc'h, S., Bayer, E., Swarup, R., Bennett, M., Mandel, T., and Kuhlemeier, C. (2008). Auxin influx carriers stabilize phyllotactic patterning. Genes Dev. **22:** 810–823.

Beemster, G.T., and Baskin, T.I. (1998). Analysis of cell division and elongation underlying the developmental acceleration of root growth in *Arabidopsis thaliana.* Plant Physiol. **116:** 1515–1526.

Benjamins, R., Malenica, N., and Luschnig, C. (2005). Regulating the regulator: the control of auxin transport. Bioessays **27:** 1246–1255.

Benjamins, R., and Scheres, B. (2008). Auxin: The looping star in plant development. Annu. Rev. Plant Biol. **59:** 443–465.

Bhalerao, R.P., Eklöf, J., Ljung, K., Marchant, A., Bennett, M., and Sandberg, G. (2002). Shoot-derived auxin is essential for early lateral root emergence in *Arabidopsis* seedlings. Plant J. **29:** 325–332.

Blilou, I., Xu, J., Wildwater, M., Willemsen, V., Paponov, I., Friml, J., Heidstra, R., Aida, M., Palme, K., and Scheres, B. (2005). The PIN auxin efflux facilitator network controls growth and patterning in *Arabidopsis* roots. Nature **433:** 39–44.

Booker, F., Burkey, K.O., Overmyer, K., and Jones, A.M. (2004). Differential responses of G-protein *Arabidopsis thaliana* mutants to ozone. New Phytol. **162:** 633–641.

Casimiro, I., Beeckman, T., Graham, N., Bhalerao, R., Zhang, H., Casero, P., Sandberg, G., and Bennett, M.J. (2003). Dissecting *Arabidopsis* lateral root development. Trends Plant Sci. **8:** 165–171.

Casimiro, I., Marchant, A., Bhalerao, R.P., Beeckman, T., Dhooge, S., Swarup, R., Graham, N., Inze, D., Sandberg, G., Casero, P.J., and Bennett, M. (2001). Auxin transport promotes *Arabidopsis* lateral root initiation. Plant Cell **13:** 843–852.

Chakravorty, D., and Botella, J.R. (2007). Over-expression of a truncated *Arabidopsis thaliana* heterotrimeric G protein γ subunit results in a phenotype similar to α and β subunit knockouts. Gene **393:** 163–170.

Chen, J.G., Gao, Y., and Jones, A.M. (2006a). Differential roles of *Arabidopsis* heterotrimeric G-protein subunits in modulating cell division in roots. Plant Physiol. **141:** 887–897.

Chen, J.G., and Jones, A.M. (2004). AtRGS1 function in *Arabidopsis thaliana.* Methods Enzymol. **389:** 338–350.

Chen, J.-G., Ullah, H., Temple, B., Liang, J., Alonso, J.M., Ecker, J., and Jones, A.M. (2006c). RACK1 mediates hormone responses and regulates multiple developmental processes in Arabidopsis. J. Exp. Bot. **57:** 2697–2708.

Chen, J.G., Willard, F.S., Huang, J., Liang, J., Chasse, S.A., Jones, A. M., and Siderovski, D.P. (2003). A seven-transmembrane RGS protein that modulates plant cell proliferation. Science **301:** 1728–1731.

Chen, S., Lin, F., Shin, M.E., Wang, F., Shen, L., and Hamm, H.E. (2008). RACK1 regulates directional cell migration by acting on Gbg at the interface with its effectors PLC beta and PI3K gamma. Mol. Biol. Cell **19:** 3909–3922.

Chen, Z., Hartmann, H.A., Wu, M.J., Friedman, E.J., Chen, J.G., Pulley, M., Schulze-Lefert, P., Panstruga, R., and Jones, A.M. (2006b). Expression analysis of the AtMLO gene family encoding plant-specific seven-transmembrane domain proteins. Plant Mol. Biol. **60:** 583–597.

Chen, Z., Noir, S., Kwaaitaal, M., Hartmann, H.A., Wu, M.J., Mudgil, Y., Sukumar, P., Muday, G., Panstruga, R., and Jones, A.M. (2009). Two seven-transmembrane domain MILDEW RESISTANCE LOCUS O proteins cofunction in *Arabidopsis* root thigmomorphogenesis. Plant Cell **21:** 1972–1991.

Clough, S.J., and Bent, A.F. (1998). Floral dip: A simplified method for Agrobacterium-mediated transformation of *Arabidopsis thaliana.* Plant J. **16:** 735–743.

Crespo, P., Xu, N., Simonds, W.F., and Gutkind, J.S. (1994). Ras-dependent activation of MAP kinase pathway mediated by G-protein βγ subunits. Nature **369:** 418–420.

Day, B., Dahlbeck, D., and Staskawicz, B.J. (2006). NDR1 interaction with RIN4 mediates the differential activation of multiple disease resistance pathways in *Arabidopsis.* Plant Cell **18:** 2782–2791.

De Smet, I., et al. (2007). Auxin-dependent regulation of lateral root positioning in the basal meristem of *Arabidopsis.* Development **134:** 681–690.

Dhanasekaran, N., Tsim, S.T., Dermott, J.M., and Onesime, D. (1998). Regulation of cell proliferation by G proteins. Oncogene **17:** 1383–1394.

Ding, L., Pandey, S., and Assmann, S.M. (2008). *Arabidopsis* extra-large G proteins (XLGs) regulate root morphogenesis. Plant J. **53:** 248–263.

Dubrovsky, J.G., Doerner, P.W., Colon-Carmona, A., and Rost, T.L. (2000). Pericycle cell proliferation and lateral root initiation in *Arabidopsis.* Plant Physiol. **124:** 1648–1657.

Dubrovsky, J.G., Rost, T.L., Colon-Carmona, A., and Doerner, P. (2001). Early primordium morphogenesis during lateral root initiation in *Arabidopsis thaliana.* Planta **214:** 30–36.

Emanuelsson, O., Nielsen, H., Brunak, S., and von Heijne, G. (2000). Predicting subcellular localization of proteins based on their N-terminal amino acid sequence. J. Mol. Biol. **300:** 1005–1016.

Fan, L.-M., Zhang, W., Chen, J.-G., Taylor, J.P., Jones, A.M., and Assmann, S.M. (2008). Abscisic acid regulation of guard-cell inwardly-rectifying K^+ channels in Gβ and RGS–deficient *Arabidopsis* lines. Proc. Natl. Acad. Sci. USA **105:** 8476–8481.

Forde, B.G. (2002). The role of long-distance signalling in plant responses to nitrate and other nutrients. J. Exp. Bot. **53:** 39–43.

Forde, B.G., and Lea, P.J. (2007). Glutamate in plants: metabolism, regulation, and signalling. J. Exp. Bot. **58:** 2339–2358.

Friml, J., Benkova, E., Blilou, I., Wisniewska, J., Hamann, T., Ljung, K., Woody, S., Sandberg, G., Scheres, B., Jurgens, G., and Palme, K. (2002). AtPIN4 mediates sink-driven auxin gradients and root patterning in *Arabidopsis.* Cell **108:** 661–673.

Fukaki, H., Okushima, Y., and Tasaka, M. (2007). Auxin-mediated lateral root formation in higher plants. Int. Rev. Cytol. **256:** 111–137.

Furukawa, I., Kurooka, S., Arisue, K., Kohda, K., and Hayashi, C. (1982). Assays of serum lipase by the "BALB-DTNB method" mechanized for use with discrete and continuous-flow analyzers. Clin. Chem. **28:** 110–113.

Geisler, M., et al. (2005). Cellular efflux of auxin catalyzed by the *Arabidopsis* MDR/PGP transporter AtPGP1. Plant J. **44:** 179–194.

Gibson, S.I. (2005). Control of plant development and gene expression by sugar signaling. Curr. Opin. Plant Biol. **8:** 93–102.

Ginalski, K., Elofsson, A., Fischer, D., and Rychlewski, L. (2003). 3D-Jury: A simple approach to improve protein structure predictions. Bioinformatics **19:** 1015–1018.

Gonzali, S., Novi, G., Loreti, E., Paolicchi, F., Poggi, A., Alpi, A., and Perata, P. (2005). A turanose-insensitive mutant suggests a role for WOX5 in auxin homeostasis in *Arabidopsis thaliana.* Plant J. **44:** 633–645.

Grieneisen, V.A., Xu, J., Maree, A.F., Hogeweg, P., and Scheres, B. (2007). Auxin transport is sufficient to generate a maximum and gradient guiding root growth. Nature **449:** 1008–1013.

Grigston, J.C., Osuna, D., Scheible, W.R., Liu, C., Stitt, M., and

Jones, A.M. (2008). D-Glucose sensing by a plasma membrane regulator of G signaling protein, AtRGS1. FEBS Lett. **582:** 3577–3584.

Guan, R.J., Ford, H.L., Fu, Y., Li, Y., Shaw, L.M., and Pardee, A.B. (2000). Drg-1 as a differentiation-related, putative metastatic suppressor gene in human colon cancer. Cancer Res. **60:** 749–755.

Gutierrez, R.A., Lejay, L.V., Dean, A., Chiaromonte, F., Shasha, D.E., and Coruzzi, G.M. (2007). Qualitative network models and genome-wide expression data define carbon/nitrogen-responsive molecular machines in *Arabidopsis.* Genome Biol. **8:** R7.

Himanen, K., Boucheron, E., Vanneste, S., de Almeida Engler, J., Inze, D., and Beeckman, T. (2002). Auxin-mediated cell cycle activation during early lateral root initiation. Plant Cell **14:** 2339–2351.

Horsman, G.P., Bhowmik, S., Seah, S.Y., Kumar, P., Bolin, J.T., and Eltis, L.D. (2007). The tautomeric half-reaction of BphD, a C–C bond hydrolase. Kinetic and structural evidence supporting a key role for histidine 265 of the catalytic triad. J. Biol. Chem. **282:** 19894–19904.

Huelsenbeck, J.P., Ronquist, F., Nielsen, R., and Bollback, J.P. (2001). Bayesian inference of phylogeny and its impact on evolutionary biology. Science **294:** 2310–2314.

Johnston, C.A., Taylor, J.P., Gao, Y., Kimple, A.J., Grigston, J.C., Chen, J.G., Siderovski, D.P., Jones, A.M., and Willard, F.S. (2007). GTPase acceleration as the rate-limiting step in *Arabidopsis* G protein-coupled sugar signaling. Proc. Natl. Acad. Sci. USA **104:** 17317–17322.

Jones, A.M. (1998). Auxin transport: Down and out and up again. Science **282:** 2201–2203.

Kachhap, S.K., Faith, D., Qian, D.Z., Shabbeer, S., Galloway, N.L., Pili, R., Denmeade, S.R., DeMarzo, A.M., and Carducci, M.A. (2007). The N-Myc Down Regulated gene1 (NDRG1) is a Rab4a effector involved in vesicular recycling of E-cadherin. PLoS One **2:** e844.

Kaneko, T., Tanaka, N., and Kumasaka, T. (2005). Crystal structures of RsbQ, a stress-response regulator in *Bacillus subtilis.* Protein Sci. **14:** 558–565.

Karimi, M., Inze, D., and Depicker, A. (2002). GATEWAY vectors for Agrobacterium-mediated plant transformation. Trends Plant Sci. **7:** 193–195.

Karthikeyan, A.S., Varadarajan, D.K., Jain, A., Held, M.A., Carpita, N. C., and Raghothama, K.G. (2007). Phosphate starvation responses are mediated by sugar signaling in *Arabidopsis.* Planta **225:** 907–918.

Kato, C., Mizutani, T., Tamaki, H., Kumagai, H., Kamiya, T., Hirobe, A., Fujisawa, Y., Kato, H., and Iwasaki, Y. (2004). Characterization of heterotrimeric G protein complexes in rice plasma membrane. Plant J. **38:** 320–331.

Kino, T., Tiulpakov, A., Ichijo, T., Chheng, L., Kozasa, T., and Chrousos, G.P. (2005). G protein β interacts with the glucocorticoid receptor and suppresses its transcriptional activity in the nucleus. J. Cell Biol. **169:** 885–896.

Krauter-Canham, R., Bronner, R., Evrard, J.L., Hahne, G., Friedt, W., and Steinmetz, A. (1997). A transmitting tissue- and pollen-expressed protein from sunflower with sequence similarity to the human RTP protein. Plant Sci. **129:** 191–202.

Kurdistani, S.K., Arizti, P., Reimer, C.L., Sugrue, M.M., Aaronson, S. A., and Lee, S.W. (1998). Inhibition of tumor cell growth by RTP/rit42 and its responsiveness to p53 and DNA damage. Cancer Res. **58:** 4439–4444.

Lachat, P., Shaw, P., Gebhard, S., van Belzen, N., Chaubert, P., and Bosman, F.T. (2002). Expression of NDRG1, a differentiation-related gene, in human tissues. Histochem. Cell Biol. **118:** 399–408.

Laemmli, U.K. (1970). Cleavage of structural proteins during the assembly of the head of bacteriophage T4. Nature **227:** 680–685.

Laskowski, M., Biller, S., Stanley, K., Kajstura, T., and Prusty, R. (2006). Expression profiling of auxin-treated *Arabidopsis* roots: Toward a molecular analysis of lateral root emergence. Plant Cell Physiol. **47:** 788–792.

Lazarescu, E., Friedt, W., Horn, R., and Steinmetz, A. (2006). Expression analysis of the sunflower SF21 gene family reveals multiple alternative and organ-specific splicing of transcripts. Gene **374:** 77–86.

Lease, K.A., Wen, J., Li, J., Doke, J.T., Liscum, E., and Walker, J.C. (2001). A mutant *Arabidopsis* heterotrimeric G-protein beta subunit affects leaf, flower, and fruit development. Plant Cell **13:** 2631–2641.

Lejay, L., Tillard, P., Lepetit, M., Olive, F., Filleur, S., Daniel-Vedele, F., and Gojon, A. (1999). Molecular and functional regulation of two NO3- uptake systems by N- and C-status of *Arabidopsis* plants. Plant J. **18:** 509–519.

Lewis, D.R., and Muday, G.K. (2009). Measurement of auxin transport in *Arabidopsis thaliana.* Nat. Protoc. **4:** 437–451.

Malamy, J.E. (2005). Intrinsic and environmental response pathways that regulate root system architecture. Plant Cell Environ. **28:** 67–77.

Malamy, J.E., and Benfey, P.N. (1997). Organization and cell differentiation in lateral roots of *Arabidopsis thaliana.* Development **124:** 33–44.

Mason, M.G., and Botella, J.R. (2001). Isolation of a novel G-protein γ-subunit from *Arabidopsis thaliana* and its interaction with Gβ^1. Biochim. Biophys. Acta **1520:** 147–153.

Mishra, B.S., Singh, M., Aggrawal, P., and Laxmi, A. (2009). Glucose and auxin signaling interaction in controlling *Arabidopsis thaliana* seedlings root growth and development. PLoS One **4:** e4502.

Moore, B., Zhou, L., Rolland, F., Hall, Q., Cheng, W.H., Liu, Y.X., Hwang, I., Jones, T., and Sheen, J. (2003). Role of the *Arabidopsis* glucose sensor HXK1 in nutrient, light, and hormonal signaling. Science **300:** 332–336.

Mravec, J., et al. (2009). Subcellular homeostasis of phytohormone auxin is mediated by the ER-localized PIN5 transporter. Nature **459:** 1136–1140.

Nakagawa, T., Kurose, T., Hino, T., Tanaka, K., Kawamukai, M., Niwa, Y., Toyooka, K., Matsuoka, K., Jinbo, T., and Kimura, T. (2007). Development of series of gateway binary vectors, pGWBs, for realizing efficient construction of fusion genes for plant transformation. J. Biosci. Bioeng. **104:** 34–41.

Nakayama, M., Kikuno, R., and Ohara, O. (2002). Protein-protein interactions between large proteins: two-hybrid screening using a functionally classified library composed of long cDNAs. Genome Res. **12:** 1773–1784.

Ohto, M.A., Hayashi, S., Sawa, S., Hashimoto-Ohta, A., and Nakamura, K. (2006). Involvement of HLS1 in sugar and auxin signaling in *Arabidopsis* leaves. Plant Cell Physiol. **47:** 1603–1611.

Ollis, D.L., et al. (1992). The αβ hydrolase fold. Protein Eng. **5:** 197–211.

Pandey, S., Chen, J.G., Jones, A.M., and Assmann, S.M. (2006). G-protein complex mutants are hypersensitive to abscisic acid regulation of germination and postgermination development. Plant Physiol. **141:** 243–256.

Pandey, S., Monshausen, G.B., Ding, L., and Assmann, S.M. (2008). Regulation of root-wave response by extra large and conventional G proteins in *Arabidopsis thaliana.* Plant J. **55:** 311–322.

Peret, B., De Rybel, B., Casimiro, I., Benkova, E., Swarup, R., Laplaze, L., Beeckman, T., and Bennett, M.J. (2009). *Arabidopsis* lateral root development: An emerging story. Trends Plant Sci. **14:** 399–408.

Peskan-Berghofer, T., Neuwirth, J., Kusnetsov, V., and Oelmuller, R. (2005). Suppression of heterotrimeric G-protein β-subunit affects anther shape, pollen development and inflorescence architecture in tobacco. Planta **220:** 737–746.

Petersson, S.V., Johansson, A.I., Kowalczyk, M., Makoveychuk, A., Wang, J.Y., Moritz, T., Grebe, M., Benfey, P.N., Sandberg, G., and

Ljung, K. (2009). An auxin gradient and maximum in the *Arabidopsis* root apex shown by high-resolution cell-specific analysis of IAA distribution and synthesis. Plant Cell **21:** 1659–1668.

Petrasek, J., et al. (2006). PIN proteins perform a rate-limiting function in cellular auxin efflux. Science **312:** 914–918.

Piquemal, D., Joulia, D., Balaguer, P., Basset, A., Marti, J., and Commes, T. (1999). Differential expression of the RTP/Drg1/Ndr1 gene product in proliferating and growth arrested cells. Biochim. Biophys. Acta **1450:** 364–373.

Price, J., Laxmi, A., St Martin, S.K., and Jang, J.C. (2004). Global transcription profiling reveals multiple sugar signal transduction mechanisms in *Arabidopsis.* Plant Cell **16:** 2128–2150.

Qu, X., Zhai, Y., Wei, H., Zhang, C., Xing, G., Yu, Y., and He, F. (2002). Characterization and expression of three novel differentiation-related genes belong to the human NDRG gene family. Mol. Cell. Biochem. **229:** 35–44.

Rebois, R.V., Robitaille, M., Gales, C., Dupre, D.J., Baragli, A., Trieu, P., Ethier, N., Bouvier, M., and Hebert, T.E. (2006). Heterotrimeric G proteins form stable complexes with adenylyl cyclase and Kir3.1 channels in living cells. J. Cell Sci. **119:** 2807–2818.

Renault, L., Negre, V., Hotelier, T., Cousin, X., Marchot, P., and Chatonnet, A. (2005). New friendly tools for users of ESTHER, the database of the α/β-hydrolase fold superfamily of proteins. Chem. Biol. Interact. **157–158:** 339–343.

Ronquist, F., and Huelsenbeck, J.P. (2003). MrBayes 3: Bayesian phylogenetic inference under mixed models. Bioinformatics **19:** 1572–1574.

Rubio, V., Bustos, R., Irigoyen, M.L., Cardona-Lopez, X., Rojas-Triana, M., and Paz-Ares, J. (2009). Plant hormones and nutrient signaling. Plant Mol. Biol. **69:** 361–373.

Salnikow, K., Blagosklonny, M.V., Ryan, H., Johnson, R., and Costa, M. (2000). Carcinogenic nickel induces genes involved with hypoxic stress. Cancer Res. **60:** 38–41.

Shaw, E., McCue, L.A., Lawrence, C.E., and Dordick, J.S. (2002). Identification of a novel class in the alpha/beta hydrolase fold superfamily: The N-myc differentiation-related proteins. Proteins **47:** 163–168.

Shimono, A., Okuda, T., and Kondoh, H. (1999). N-myc-dependent repression of ndr1, a gene identified by direct subtraction of whole mouse embryo cDNAs between wild type and N-myc mutant. Mech. Dev. **83:** 39–52.

Smith, D.L., and Fedoroff, N.V. (1995). LRP1, a gene expressed in lateral and adventitious root primordia of *Arabidopsis.* Plant Cell **7:** 735–745.

Stals, H., and Inze, D. (2001). When plant cells decide to divide. Trends Plant Sci. **6:** 359–364.

Sugiki, T., Murakami, M., Taketomi, Y., Kikuchi-Yanoshita, R., and Kudo, I. (2004a). N-myc downregulated gene 1 is a phosphorylated protein in mast cells. Biol. Pharm. Bull. **27:** 624–627.

Sugiki, T., Taketomi, Y., Kikuchi-Yanoshita, R., Murakami, M., and Kudo, I. (2004b). Association of N-myc downregulated gene 1 with heat-shock cognate protein 70 in mast cells. Biol. Pharm. Bull. **27:** 628–633.

Temple, B.R., and Jones, A.M. (2007). The plant heterotrimeric G-protein complex. Annu. Rev. Plant Biol. **58:** 249–266.

Thompson, J.D., Gibson, T.J., Plewniak, F., Jeanmougin, F., and Higgins, D.G. (1997). The CLUSTAL_X windows interface: Flexible strategies for multiple sequence alignment aided by quality analysis tools. Nucleic Acids Res. **25:** 4876–4882.

Trusov, Y., Rookes, J.E., Chakravorty, D., Armour, D., Schenk, P.M., and Botella, J.R. (2006). Heterotrimeric G proteins facilitate *Arabidopsis* resistance to necrotrophic pathogens and are involved in jasmonate signaling. Plant Physiol. **140:** 210–220.

Trusov, Y., Rookes, J.E., Tilbrook, K., Chakravorty, D., Mason, M.G., Anderson, D., Chen, J.G., Jones, A.M., and Botella, J.R. (2007). Heterotrimeric G protein γ subunits provide functional selectivity in Gβγ dimer signaling in *Arabidopsis.* Plant Cell **19:** 1235–1250.

Trusov, Y., Zhang, W., Assmann, S.M., and Botella, J.R. (2008). Gγ1 + Gγ2 not equal to Gβ: Heterotrimeric G protein Gγ-deficient mutants do not recapitulate all phenotypes of Gβ-deficient mutants. Plant Physiol. **147:** 636–649.

Tsukada, S., Simon, M.I., Witte, O.N., and Katz, A. (1994). Binding of βγ subunits of heterotrimeric G proteins to the PH domain of Bruton tyrosine kinase. Proc. Natl. Acad. Sci. USA **91:** 11256–11260.

Ueda, M., Koshino-Kimura, Y., and Okada, K. (2005). Stepwise understanding of root development. Curr. Opin. Plant Biol. **8:** 71–76.

Ullah, H., Chen, J.G., Temple, B., Boyes, D.C., Alonso, J.M., Davis, K.R., Ecker, J.R., and Jones, A.M. (2003). The β-subunit of the *Arabidopsis* G protein negatively regulates auxin-induced cell division and affects multiple developmental processes. Plant Cell **15:** 393–409.

Ullah, H., Chen, J.G., Young, J.C., Im, K.H., Sussman, M.R., and Jones, A.M. (2001). Modulation of cell proliferation by heterotrimeric G protein in *Arabidopsis.* Science **292:** 2066–2069.

Ulmasov, T., Murfett, J., Hagen, G., and Guilfoyle, T.J. (1997). Aux/IAA proteins repress expression of reporter genes containing natural and highly active synthetic auxin response elements. Plant Cell **9:** 1963–1971.

van Belzen, N., Dinjens, W.N., Eussen, B.H., and Bosman, F.T. (1998). Expression of differentiation-related genes in colorectal cancer: Possible implications for prognosis. Histol. Histopathol. **13:** 1233–1242.

Wang, S., Narendra, S., and Fedoroff, N. (2007). Heterotrimeric G protein signaling in the *Arabidopsis* unfolded protein response. Proc. Natl. Acad. Sci. USA **104:** 3817–3822.

Weerasinghe, R.R., Swanson, S.J., Okada, S.F., Garrett, M.B., Kim, S.Y., Stacey, G., Boucher, R.C., Gilroy, S., and Jones, A.M. (2009). Touch induces ATP release in *Arabidopsis* roots that is modulated by the heterotrimeric G-protein complex. FEBS Lett. **583:** 2521–2526.

Wetmore, R.H., and Rier, J.P. (1963). Experimental induction of vascular tissues in callus of angiosperms. Am. J. Bot. **50:** 418–430.

Wetmore, R.H., and Sorokin, S. (1955). On the differentiation of xylem. J. Arnold Arbor. **36:** 305–317.

Wisniewska, J., Xu, J., Seifertova, D., Brewer, P.B., Ruzicka, K., Blilou, I., Rouquie, D., Benkova, E., Scheres, B., and Friml, J. (2006). Polar PIN localization directs auxin flow in plants. Science **312:** 883.

Xu, J., Wu, D., Slepak, V.Z., and Simon, M.I. (1995). The N terminus of phosducin is involved in binding of βγ subunits of G protein. Proc. Natl. Acad. Sci. USA **92:** 2086–2090.

Yang, J., Koga, Y., Nakano, H., and Yamane, T. (2002). Modifying the chain-length selectivity of the lipase from *Burkholderia cepacia* KWI-56 through in vitro combinatorial mutagenesis in the substrate-binding site. Protein Eng. **15:** 147–152.

Yeger-Lotem, E., Sattath, S., Kashtan, N., Itzkovitz, S., Milo, R., Pinter, R.Y., Alon, U., and Margalit, H. (2004). Network motifs in integrated cellular networks of transcription-regulation and protein-protein interaction. Proc. Natl. Acad. Sci. USA **101:** 5934–5939.

Zazimalova, E., Krecek, P., Skupa, P., Hoyerova, K., and Petrasek, J. (2007). Polar transport of the plant hormone auxin - the role of PIN-FORMED (PIN) proteins. Cell. Mol. Life Sci. **64:** 1621–1637.

Zhang, H., Rong, H., and Pilbeam, D. (2007). Signalling mechanisms underlying the morphological responses of the root system to nitrogen in *Arabidopsis thaliana.* J. Exp. Bot. **58:** 2329–2338.

Zhao, Q., Kawano, T., Nakata, H., Nakajima, Y., Nakajima, S., and

Kozasa, T. (2003). Interaction of G protein β subunit with inward rectifier K^+ channel Kir3. Mol. Pharmacol. **64:** 1085–1091.

Zhou, R.H., Kokame, K., Tsukamoto, Y., Yutani, C., Kato, H., and Miyata, T. (2001). Characterization of the human NDRG gene family: A newly identified member, NDRG4, is specifically expressed in brain and heart. Genomics **73:** 86–97.

QUERIES -pc065557

[AQ1] Journal style is to cite the full Latin name at first use in the Abstract, text, and Methods. Please confirm or amend insertions made throughout the article.

[AQ2] Please verify the definitions inserted for CFP, GFP, and GST.

[AQ3] DJS: This paragraph, and three paragraphs below, are not tagged correctly.

[AQ4] Please replace NAA with the full term both times in the article.

[AQ5] Please replace NIGMS and DFG with the full names here.